

General Disclaimer

One or more of the Following Statements may affect this Document

- This document has been reproduced from the best copy furnished by the organizational source. It is being released in the interest of making available as much information as possible.
- This document may contain data, which exceeds the sheet parameters. It was furnished in this condition by the organizational source and is the best copy available.
- This document may contain tone-on-tone or color graphs, charts and/or pictures, which have been reproduced in black and white.
- This document is paginated as submitted by the original source.
- Portions of this document are not fully legible due to the historical nature of some of the material. However, it is the best reproduction available from the original submission.

CR-137860

NASA CONTRACTOR REPORT
A SINGLE AXIS STUDY OF
FLIGHT SIMULATOR KINEMATICS
BY DIFFERENCE TECHNIQUES

(NASA-CR-137860) A SINGLE AXIS STUDY OF
FLIGHT SIMULATOR KINEMATICS BY DIFFERENCE
TECHNIQUES (Computer Sciences Corp.,
Mountain View, Calif.) 47 p HC \$4.00

N76-22218

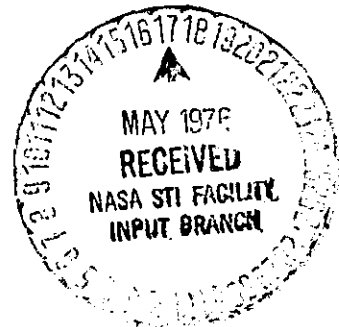
Unclass
28370

CSCI 14B G3/09

Larry D. Webster

Prepared by

COMPUTER SCIENCES CORPORATION
Mountain View, California
for AMES RESEARCH CENTER
April, 1976



1. Report No. NASA CR-137860		2. Government	3. Recipient's Catalog No.
4. Title and Subtitle A Single Axis Study of Flight Simulator Kinematics By Difference Techniques		Report Date May 1976 Performing Organization Code	
7. Author(s) Larry D. Webster		8. Performing Organization Report No.	
9. Performing Organization Name and Address Computer Sciences Corporation Mountain View, California		10. Work Unit No.	
		11. Contract or Grant No. NAS-2-7806	
12. Sponsoring Agency Name and Address National Aeronautics and Space Administration, Washington, D. C. 20546		13. Type of Report and Period Covered Contract Report	
		14. Sponsoring Agency Code	
15. Supplementary Notes			
16. Abstract <p>The kinematic parameters of position, velocity, and acceleration of a flight simulator may be calculated by knowing the distance between two or more points on an axis and the time the simulator takes to traverse the space between each set of points. These parameters are calculated through the use of difference techniques. Given the true kinematic response of the simulator to computer generated commands, the entire motion system loop may be calibrated, and system operability verified.</p>			
17. Key Words (Supplied by Author(s)) Simulator Kinematics Difference Techniques		Distribution Statement Unclassified - Unlimited Cat. 05	
19. Security Classification of this report Unclassified		20. Security Classification of this report Unclassified	
		42	

TABLE OF CONTENTS

	<u>Page</u>
LIST OF SYMBOLS	i
SUMMARY	ii
Introduction	1
Methodology	2
Position Technique	6
Velocity Technique	8
Acceleration Technique	10
Inherent Errors	13
KMS Evaluation	15
Introduction	15
Position Measurements	15
Velocity Measurements	17
Drive Signals	17
Simulator Response	18
Tachometer Readings	18
Servo Response	28
Acceleration Measurement	31
Conclusions and Recommendations	39

LIST OF SYMBOLS

a	Generalized acceleration
KMS	Kinematic Measurement System
FSAA	Flight Simulator for Advanced Aircraft
Z axis	The vertical axis of the FSAA
DAC	Digital to Analog Converter
A/D	Analog to Digital Converter
IC	Initial condition position
z_n	Position of sensor n ; $n=1,2,3,4,5$
t_n	Time of passage past sensor n , $n=1,2,3,4,5$
$\bar{z}_{n,n+1}$	Average velocity between sensors n and $n+1$
\dot{z}_s	Instantaneous simulator velocity
\dot{z}_d	Instantaneous velocity drive command
\dot{z}_f	Instantaneous tachometer indicated velocity
$\bar{z}_{n,n+2}$	Average acceleration between sensors n and $n+2$
\ddot{z}_s	Instantaneous simulator acceleration
\ddot{z}_f	Instantaneous accelerometer indicated acceleration

**A SINGLE AXIS STUDY OF
FLIGHT SIMULATOR KINEMATICS
BY DIFFERENCE TECHNIQUES**

by

Larry D. Webster

SUMMARY

The use of discrete motion parameters evaluated by difference techniques can provide useful information concerning continuous flight simulator kinematics at the NASA-Ames Research Center. In particular it can provide overall system calibration of the acceleration, velocity and position parameters of the simulator, as well as precisely measure simulator motion performance capabilities. This paper describes the difference methodology and presents the results of its implementation on the vertical axis of a six degree of freedom flight simulator.

Introduction

A technique was developed to measure and calibrate the kinematic responses of a flight motion simulator to computer requested motion commands. Preliminary tests with this KINEMATIC MEASUREMENT SYSTEM (KMS) made on the vertical (Z) axis of the Flight Simulator for Advanced Aircraft (FSAA) (See Figure 1) at NASA-Ames Research Center, determined that the technique is both feasible and useful. At discrete points in time, motion drive signals to, and simulator kinematic response signals from the Z axis follow-up systems are compared with values provided by the KMS for those times. Absolute differences between the drive/follow-up and KMS values can then be used to verify the operability of and calibrate the entire motion system loop, including digital computer scaling factors, digital to analog converters, motion drive servos, position, velocity, and acceleration sensors, and analog to digital converters. Non-linearities in the motion and follow-up systems are also detectible via this technique.

REPRODUCED FROM THE
ORIGINAL PAGE IN FORM

FLIGHT SIMULATOR FOR ADVANCED AIRCRAFT

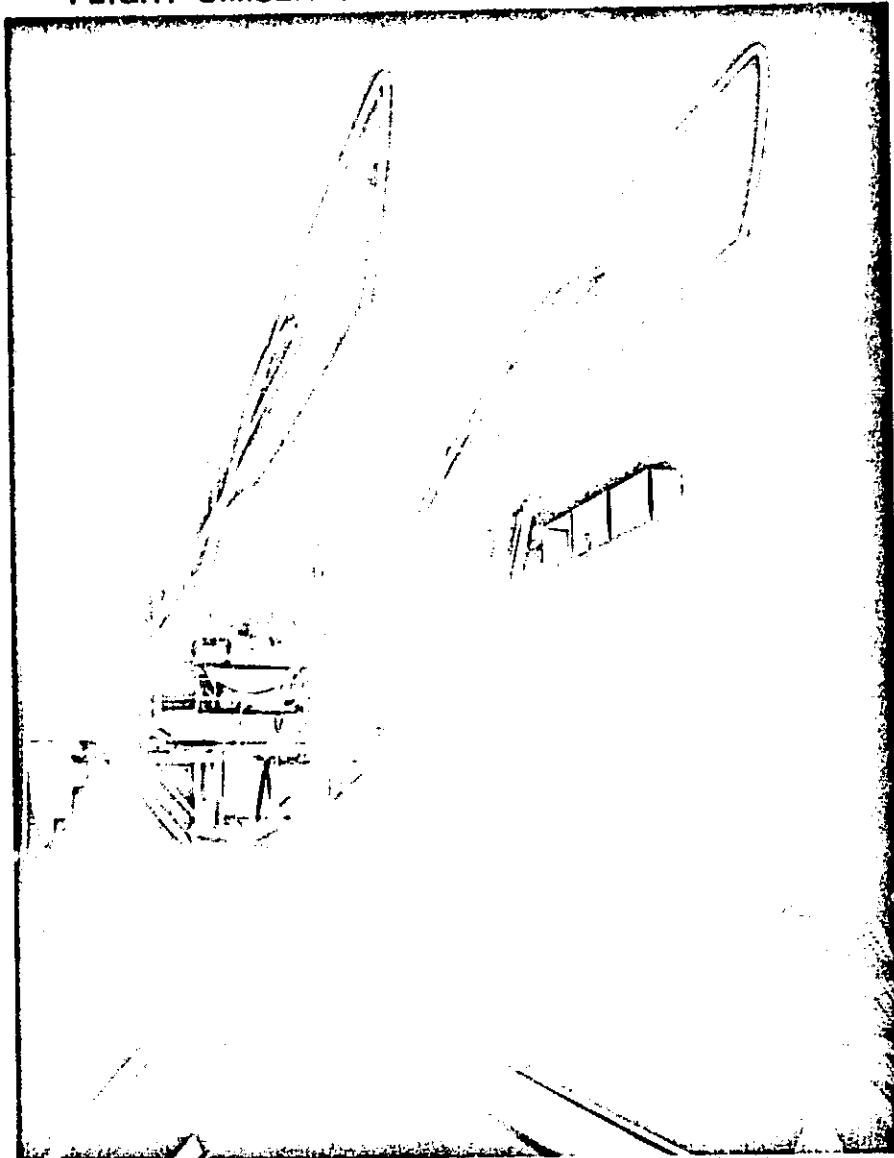


Figure 1

Methodology

In order to measure the kinematic responses of the Flight Simulator for Advanced Aircraft (FSAA) by the difference technique described herein, a system is required which would sense cab position with respect to time. As the end purpose of the Kinematic Measurement System (KMS) is to provide a kinematic calibration of the FSAA, the position sensing element of the system must be stable and invariant subsequent to an initial calibration. Mechanical sensors were not considered as they are subject to long term wear, and would require semi-frequent recalibration. Optical and magnetic components were considered for use as the position sensing element as they have no mechanically interactive parts and therefore would not be subject to wear.

An optical sensor was selected for use in the preliminary tests on the Z axis due to its ease of mechanization and calibration. The sensor is a photo transistor with a 0.17 radian angular field of view with the sensor mounted on a copper plate. A round copper tube of 0.25 cm inside diameter and 0.635 cm in length is placed over the sensor to reduce the angular field of view and eliminate any stimulus of the element by background radiation (See Figure 2). Five of these sensor assemblies were mounted on an aluminum rail approximately 25.4 cm apart (See Figure 3). The true distance between sensors was determined through an optical/electrical technique to an accuracy of ± 0.025 cm. As shown in Figure 3, the rail assembly was mounted on the fixed base of the Z axis parallel and equidistant to the Z axis direction of motion.

REPRODUCIBILITY OF THE
ORIGINAL TEXT IS POOR

SENSOR ASSEMBLY

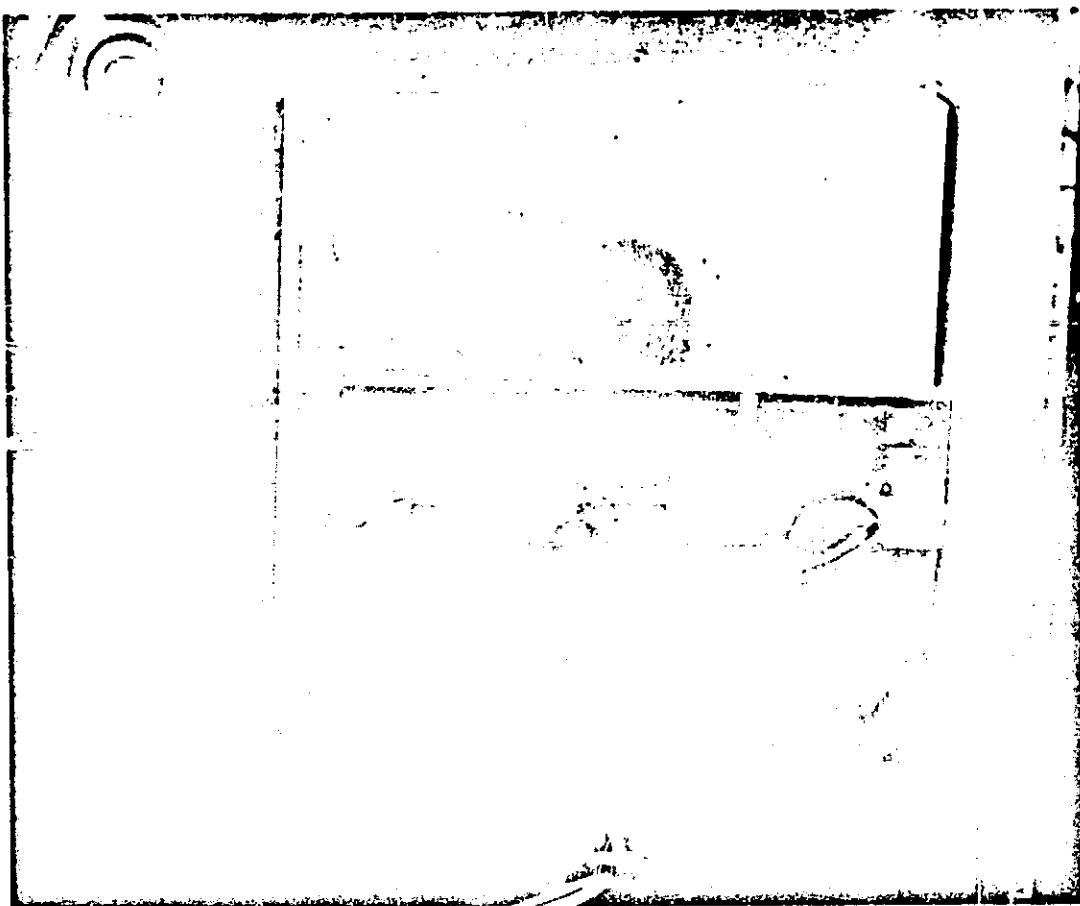


Figure 2

SENSOR ASSEMBLY MOUNTING

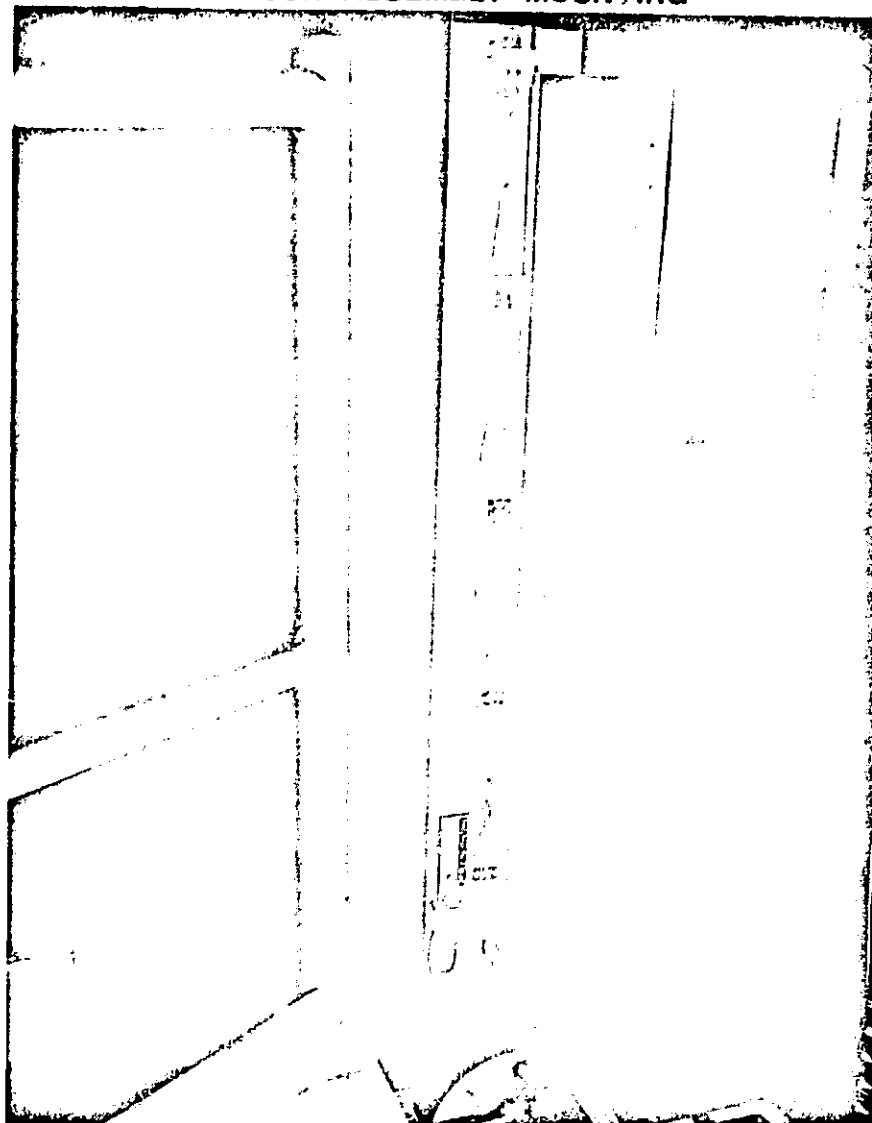


Figure 3

The kinematics of the simulator are controlled by a Xerox Sigma 8 computing system. Motion of the FSAA is achieved through input of a signal of computer derived amplitude and polarity to a velocity drive servo system. Position and acceleration are programmed parameters. Constant inputs cause constant velocity, while ramp inputs cause constant acceleration. As the FSAA travels from top to bottom, or bottom to top of the Z axis, the lamp passes each sensor in turn. When a sensor becomes activated, its position on the rail is encoded and sent to the Sigma 8 via a real time interrupt, along with the relative time of passage of the lamp past the sensor. The time for the first sensor passed is always 0.00 seconds, and some incremental time later for all other sensors, depending on simulator velocity. See Figure 4 for a block diagram showing the FSAA motion system loop and its interaction with the KMS. Upon receipt of the interrupt and data from the KMS, the computer reads the current values of the velocity drive DAC, drive amplifier, and position, velocity, and acceleration follow-up signals.

After the passage of the cab from its initial condition position past all five sensors, the computer has stored a data set of the relative time of passage of the cab past five discrete points, the distance between each of the points, and the values of the drive and follow-up signals at these times. With this data, the following information can be determined about the cab kinematics in position, velocity and acceleration.

Position Technique

The position of any sensor z_n from the center position of the axis is

KINEMATIC MEASUREMENT SYSTEM / Z - AXIS MOTION SYSTEM BLOCK DIAGRAM

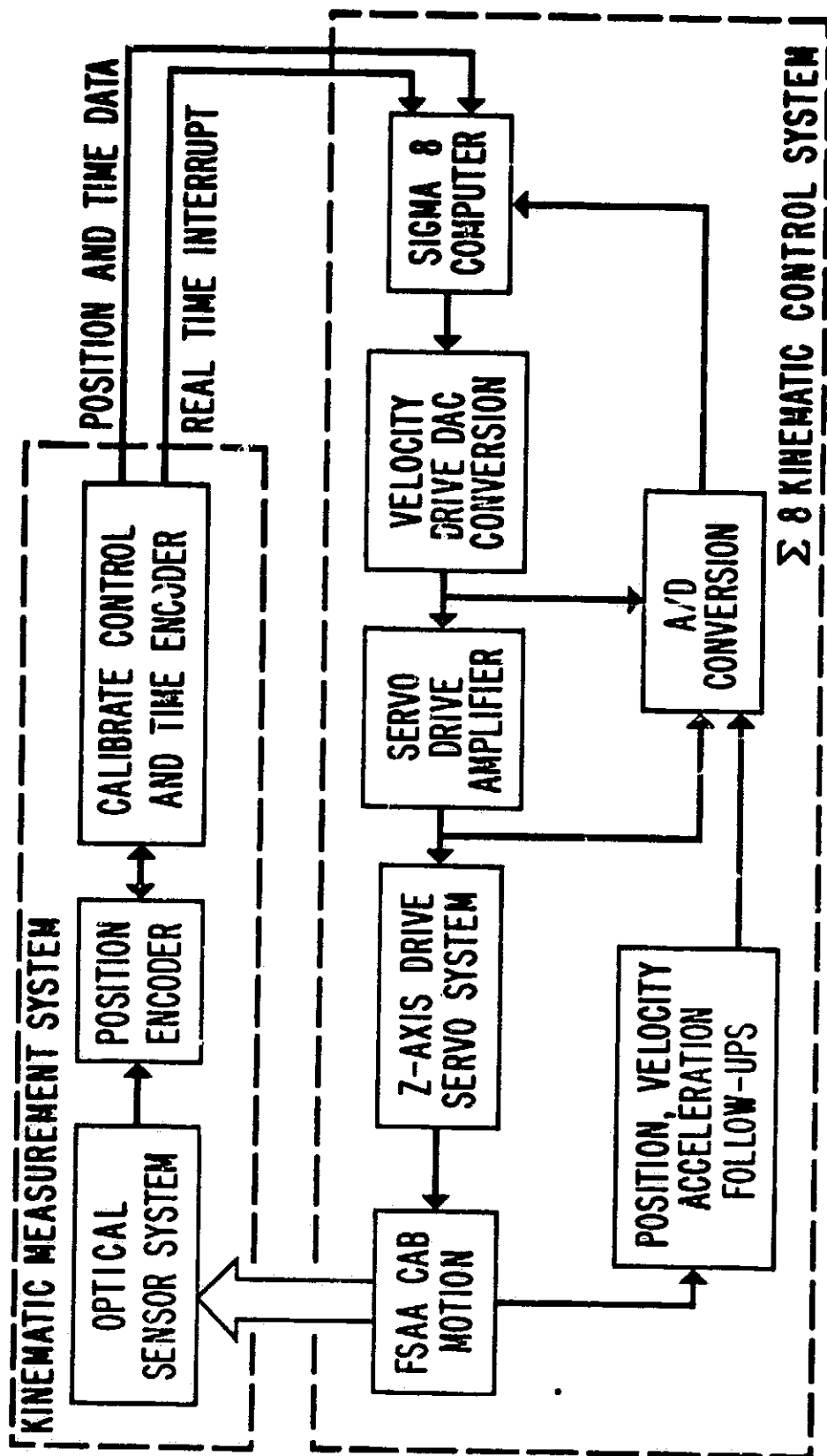


FIGURE 4

listed below. The bottom sensor has arbitrarily been labeled z_1 , and the top sensor z_5 . Positions higher than center position are positive while those below center position are negative. Thus, center position is 0.00 cm on the axis, and the position of the sensors are:

(1) $z_1 = -67.94$ cm

(2) $z_2 = -42.76$ cm

(3) $z_3 = -17.20$ cm

(4) $z_4 = +8.53$ cm

(5) $z_5 = +33.89$ cm

Values from the position follow-up circuit taken as the simulator passes a sensor can be compared with its known location on any run to calibrate the position follow-up system. The location of z_1 , the reference sensor, was arbitrarily made to agree with the value taken from the position follow-up system for that sensor.

Velocity Technique

Tests for constant velocity were performed by positioning the simulator at the top or bottom of the Z axis. A velocity step was input to the servo system of an appropriate sign and magnitude to cause the simulator to accelerate from a stop and move through the sensor test area with a velocity corresponding to the servo system's interpretation of the step input. All constant velocity tests were performed such that the simulator should not be accelerating in the test area.

Subsequent to a run, the computer divides the distance between two sen-

sensor points by the time it took the cab to travel that distance $[(t_{n+1}-t_n)$ where n is the sensor number]. This provides the average velocity, $\bar{z}_{n,n+1}$, between those two points. For small accelerations, this average velocity is approximately equal to the instantaneous velocity of the simulator \dot{z}_s , at any point between the two sensors. A comparison of values may then be made between the instantaneous velocity values of the drive command \dot{z}_d , the tachometer follow-up, \dot{z}_f , and the average velocity calculated by the KMS. The relationship may be expressed as:

$$(6) \quad \dot{z}_f \stackrel{?}{=} \dot{z}_s \approx \bar{z}_{n,n+1} = \frac{z_{n+1} - z_n}{t_{n+1} - t_n} \quad \text{as } a \rightarrow 0$$

$$(7) \quad \dot{z}_d \stackrel{?}{=} \dot{z}_s \approx \bar{z}_{n,n+1} = \frac{z_{n+1} - z_n}{t_{n+1} - t_n} \quad \text{as } a \rightarrow 0$$

The KMS provides four average velocity data points from the five sensors. For test runs with moderate constant velocity commands, graphs of the average velocity show that the acceleration is small and reasonably constant.

If the acceleration is constant but not necessarily small, there is a point in space, z_a , between two sensors where the instantaneous simulator velocity, \dot{z}_s , is equal to the average velocity, $\bar{z}_{n,n+1}$, of the simulator between those two sensors. This point is located at:

$$(8) \quad z_a = z_n + 1/4 (z_{n+1} - z_n), \quad a = \text{Constant}$$

Simply stated, the average simulator velocity, $\bar{z}_{n,n+1}$, between two sensors

n and (n+1) equals the instantaneous simulator velocity \dot{z}_s , when the simulator's position is one quarter of the distance from sensor n to sensor (n+1). All graphs of the velocity tests show a reasonably constant acceleration component. Therefore, equation (8) is used to locate the position of $\bar{z}_{n,n+1}$. By connecting the four points on a graph of $\bar{z}_{n,n+1}$ versus position on the Z axis (where the position of each $\bar{z}_{n,n+1}$ is located at the corresponding z_a), the graph becomes an approximately accurate plot of \dot{z}_s versus position. Comparison of this graph to a plot of \dot{z}_d or \dot{z}_f , shows a difference between the plots which represents the error in the simulator velocity to commanded velocity, or tachometer indicated velocity to true simulator velocity.

Acceleration Technique

Acceleration tests were performed in a manner similar to velocity tests. The simulator was stopped at the top or bottom of the Z axis and accelerated into the sensor area by input of an appropriate ramp signal into the velocity drive servo system. All tests were run such that the simulator should be moving with constant acceleration through the sensor area.

Subsequent to a run, the computer has available the point in time the simulator passed each sensor, and the distance between sensors. For constant acceleration, velocity is changing linearly with time (See Figure 5). The average velocity between two sensors is:

$$(9) \quad \bar{z}_{n,n+1} = \frac{z_{n+1} - z_n}{t_{n+1} - t_n}$$

and

$$(10) \quad z_{n+1,n+2} = \frac{z_{n+2} - z_{n+1}}{t_{n+2} - t_{n+1}}$$

As can be seen from inspection of Figure 5, under constant acceleration conditions, the instantaneous simulator velocity \dot{z}_s at the point halfway in time ($\frac{t_{n+1} + t_n}{2}$) between two sensors is equal to the average velocity between the two sensors or;

$$(11) \quad \dot{z}_{s1} = \bar{\dot{z}}_{n,n+1} \text{ when } t = \frac{t_{n+1} + t_n}{2}$$

$$(12) \quad \dot{z}_{s2} = \bar{\dot{z}}_{n+1,n+2} \text{ when } t = \frac{t_{n+2} + t_{n+1}}{2}$$

By knowing the instantaneous velocity of any two points and the time between them, the average simulator acceleration between the two points can be calculated by:

$$(13) \quad \bar{\ddot{z}}_{n,n+2} = \frac{\left(\begin{array}{l} \text{Instantaneous velocity} \\ \text{at average time between} \\ \text{sensors (n+2) and (n+1)} \end{array} \right) - \left(\begin{array}{l} \text{Instantaneous velocity} \\ \text{at average time between} \\ \text{sensors (n+1) and (n)} \end{array} \right)}{\left(\begin{array}{l} \text{Average time between} \\ \text{sensors (n+2) and (n+1)} \end{array} \right) - \left(\begin{array}{l} \text{Average time between} \\ \text{sensors (n+1) and (n)} \end{array} \right)}$$

$$(14) \quad \bar{\ddot{z}}_{n,n+2} = \frac{\left(\frac{z_{n+2} - z_{n+1}}{t_{n+2} - t_{n+1}} - \frac{z_{n+1} - z_n}{t_{n+1} - t_n} \right)}{\left(\frac{t_{n+2} + t_{n+1}}{2} - \frac{t_{n+1} + t_n}{2} \right)}$$

or

$$(15) \quad \bar{\ddot{z}}_{n,n+2} = \frac{2 \left(\frac{z_{n+2} - z_{n+1}}{t_{n+2} - t_{n+1}} - \frac{z_{n+1} - z_n}{t_{n+1} - t_n} \right)}{t_{n+2} - t_n} = \frac{2 (\bar{\dot{z}}_{n+1,n+2} - \bar{\dot{z}}_{n,n+1})}{t_{n+2} - t_n}$$

SIMULATOR VELOCITY VS TIME; ACCELERATION CONSTANT

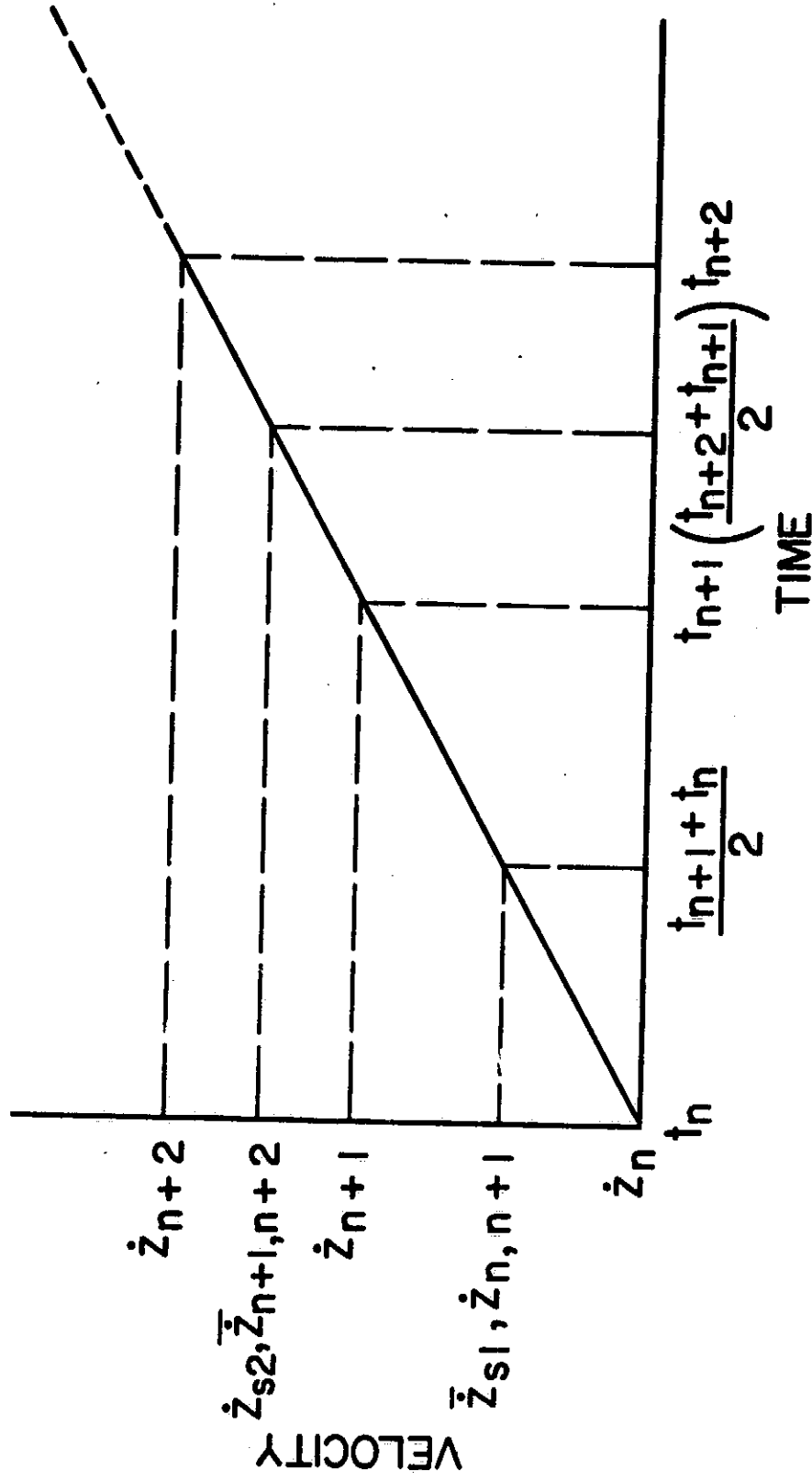


FIGURE 5

The KMS provides three average acceleration data points from the five sensors using equation (15), which provides an exact value for \bar{z}_s when simulator acceleration is constant.

$$(16) \quad \ddot{\bar{z}}_s = \ddot{\bar{z}}_{n,n+2}, \quad \ddot{\bar{z}}_s = \text{constant}$$

By connecting the three points on a graph of $\ddot{\bar{z}}_{n,n+2}$ versus position on the Z axis, the constancy of $\ddot{\bar{z}}_{n,n+2}$ can be determined. If the slope of the line is zero or reasonably small (as is true for many of the acceleration tests), this graph approximating $\ddot{\bar{z}}_s$ may be compared to graphs of the accelerometer follow-up values, \ddot{z}_f , and acceleration drive, \ddot{z}_d , versus position. The difference between the graphs represents the error in true simulator acceleration to commanded simulator acceleration, and accelerometer indicated acceleration to true simulator acceleration.

Inherent Errors

There exists a finite difference between the time a sensor is passed and the time the follow-up system is measured by the computer. During this period, follow-up values may change slightly from their value at the sensor time. This difference in time, or computer latency, has been empirically determined to average seven milliseconds.

For the position follow-up system the error introduced by the computer latency is only 0.74 cm at velocities of 183 cm./sec. or 0.4%. For velocities less than 122 cm./sec., noise present in the position follow-up system masks any error in the position readings due to latency. For the tachometer and accelerometer follow-up systems, the latency error is not significant for

velocity readings during constant velocity tests or for acceleration readings during constant acceleration tests respectively as the follow-up sensor should not be changing value in the test area.

KMS Evaluation

Introduction

An examination of the FSAA Z axis drive, servo and follow-up system was accomplished in order to evaluate the ability of the KMS to measure FSAA continuous kinematic parameters through the difference technique. Tests were made of the system at computer commands of constant velocities ranging from ± 3 cm./sec. to ± 274 cm./sec. and constant accelerations ranging from ± 3 cm./sec.² to ± 366 cm./sec.² Positive velocities and accelerations represent motion from the top to the bottom of the Z axis, while negative velocities and accelerations represent motion from the bottom to the top of the Z axis. Results from these tests are presented below.

Position Measurement

Table 1 shows the position of each sensor as taken from the position follow-up system as each sensor is activated. The effect of latency has been removed from the numbers. Subtracting the true location of each sensor from the

Sensor #	Follow-up Positions (cm.)
5	+42.92
4	+15.41
3	-14.91
2	-42.37
1	-67.94

Table 1
Position Follow-up Sensor Locations

value provided by the position follow-up system provides the error of the position follow-up system. This is shown in Table 2.

Sensor #	Follow-up Error (cm.)
5	9.03
4	6.88
3	2.29
2	0.39
1	0.00

Table 2
Position Follow-up Error

Figure 6 shows a plot of follow-up error versus position on the Z axis using sensor #1 as a reference.

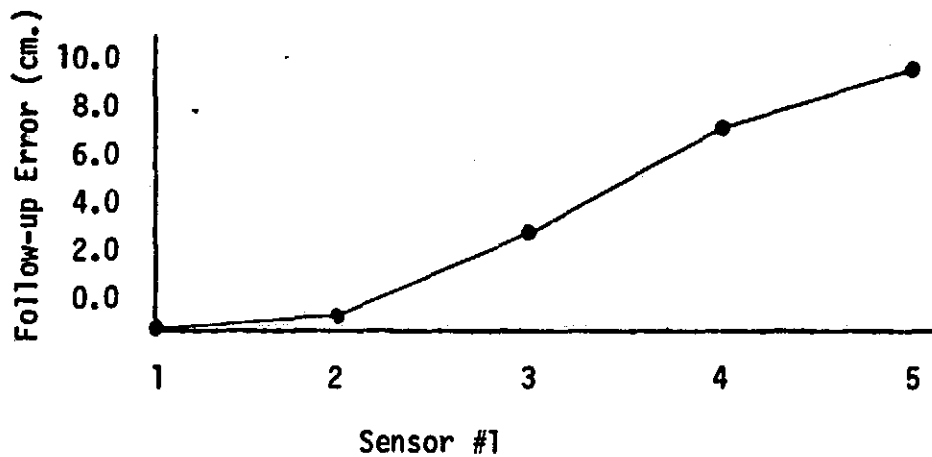
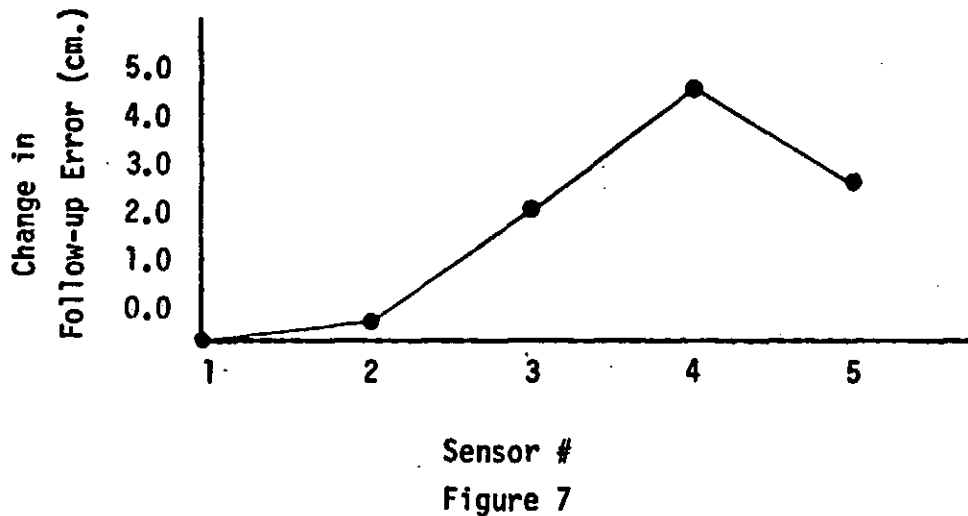


Figure 6

Position Follow-up Error versus Position

Figure 7 shows the change in error versus position. Notice that the curve shows a large increase in the error growth occurring between sensors #3 and

and #4, accompanied by a change in slope between sensor #4 and #5.



Change in Follow-up Error versus Position

Because of the accuracy of the calibration of the KMS, and because this variation between the position follow-up and the KMS is consistent and repeatable, it may be stated that the KMS has detected an inaccuracy in the Z axis position follow-up system which has its most pronounced effect in the space between sensors #3 and #4. The additional error introduced while traveling the 25.7 cm. between these two sensors is 4.6 cm. or approximately an 18% change.

Velocity Measurements

Drive Signals

Table 3 displays the drive signals for several randomly selected velocity commands as required by the KMS software. As can be seen, transmission of the required command was accomplished by the velocity drive DAC and the servo drive amplifier within reasonable limits.

Software Required Velocity (cm./sec.)	Velocity Drive DAC Conversion (cm./sec.)	Servo Drive Ampli- fier (cm./sec.)
3.05	3.01	3.14
7.62	7.51	7.68
30.48	30.59	30.21
91.44	91.56	90.53
152.40	152.37	150.85
182.88	182.90	181.62
-3.05	-3.15	-3.02
-15.24	-15.23	-15.30
-60.96	-60.69	-60.94
-121.92	-121.86	-120.67
-182.88	-182.80	-181.15

Table 3
Drive Signal Response

Simulator Response

Figures 8 through 16 display the results of constant velocity command tests for various commands in the range of ± 3.0 cm./sec. to ± 183 cm./sec. For positive velocities, the simulator was started approximately 76 cm. above sensor #5, and travel was downward. For negative velocities the simulator was started approximately 61 cm. below the bottom sensor and travel was upward. In either direction, the simulator should not have been accelerating in the test area.

Tachometer Readings

For commands through ± 61 cm./sec., the KMS measurements form straight

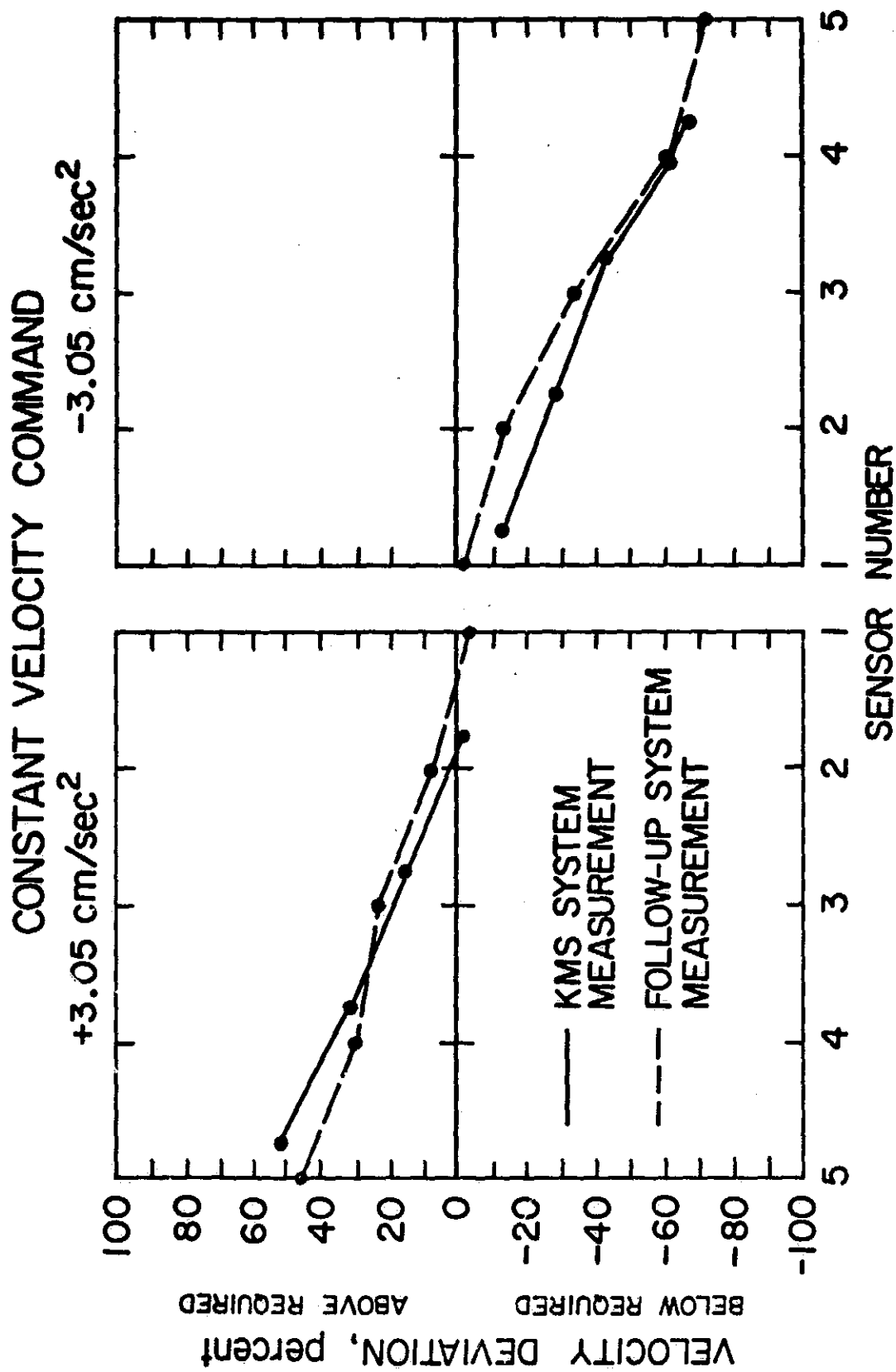


FIGURE 8

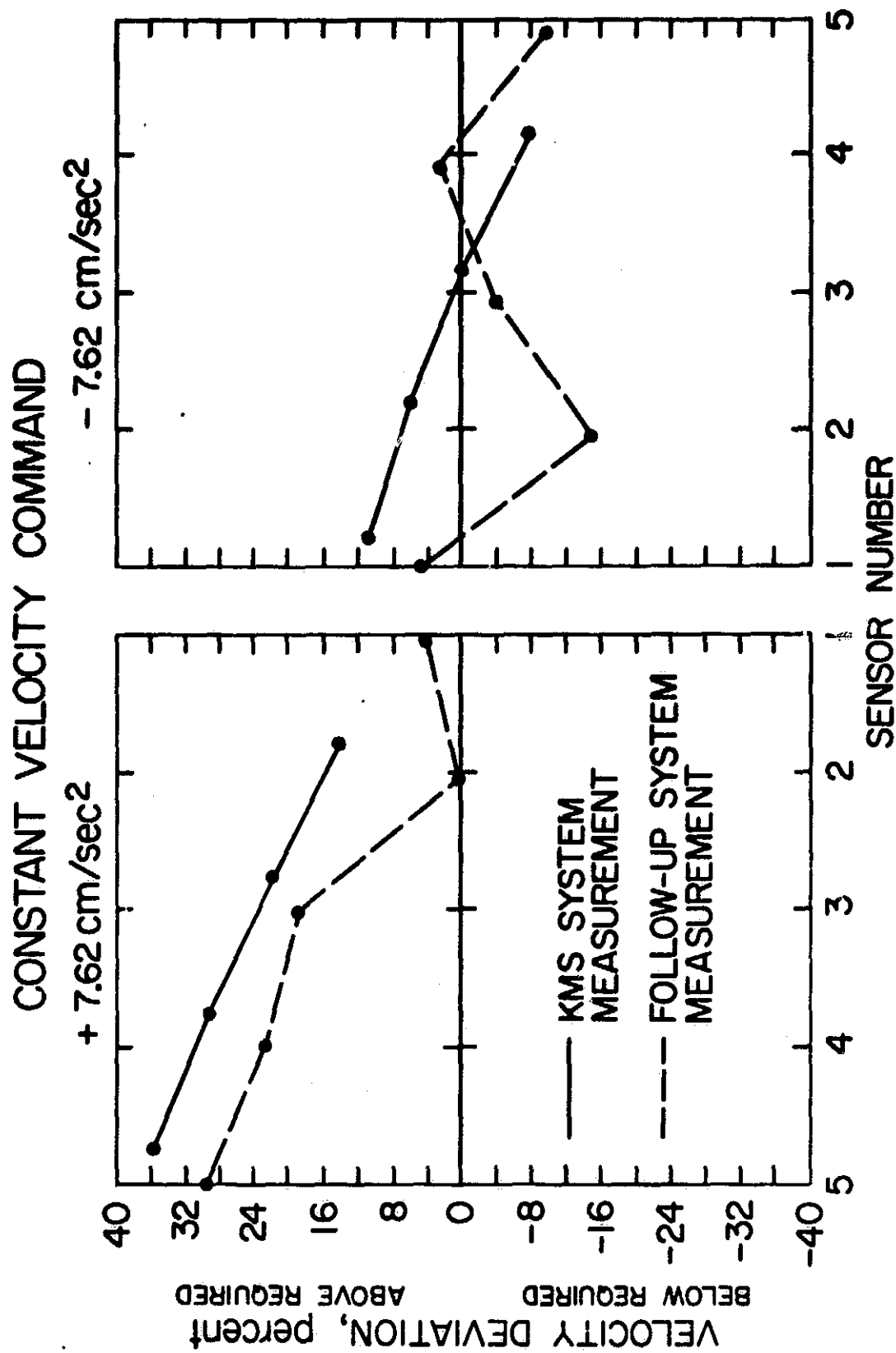


FIGURE 9

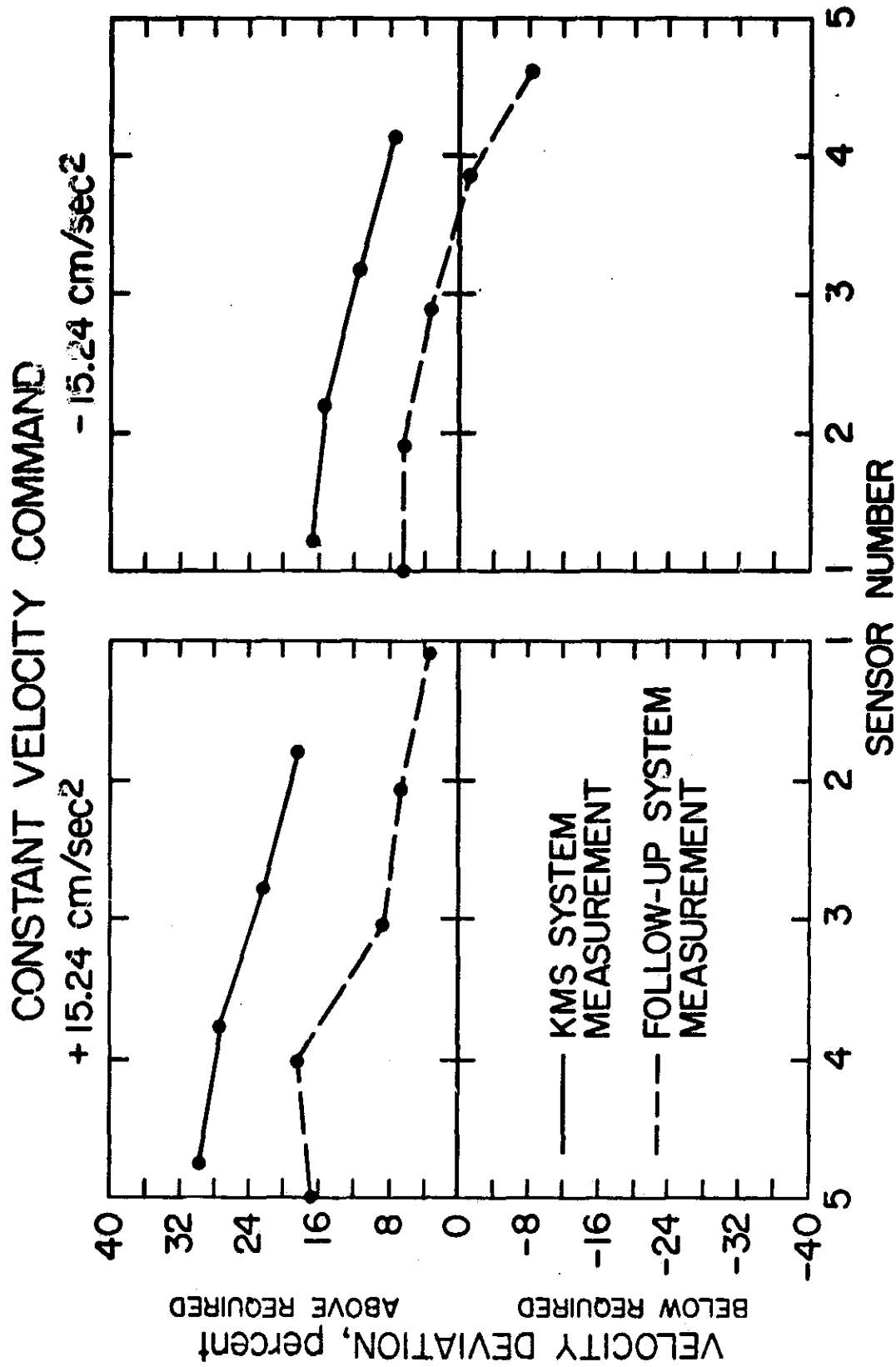


FIGURE 10

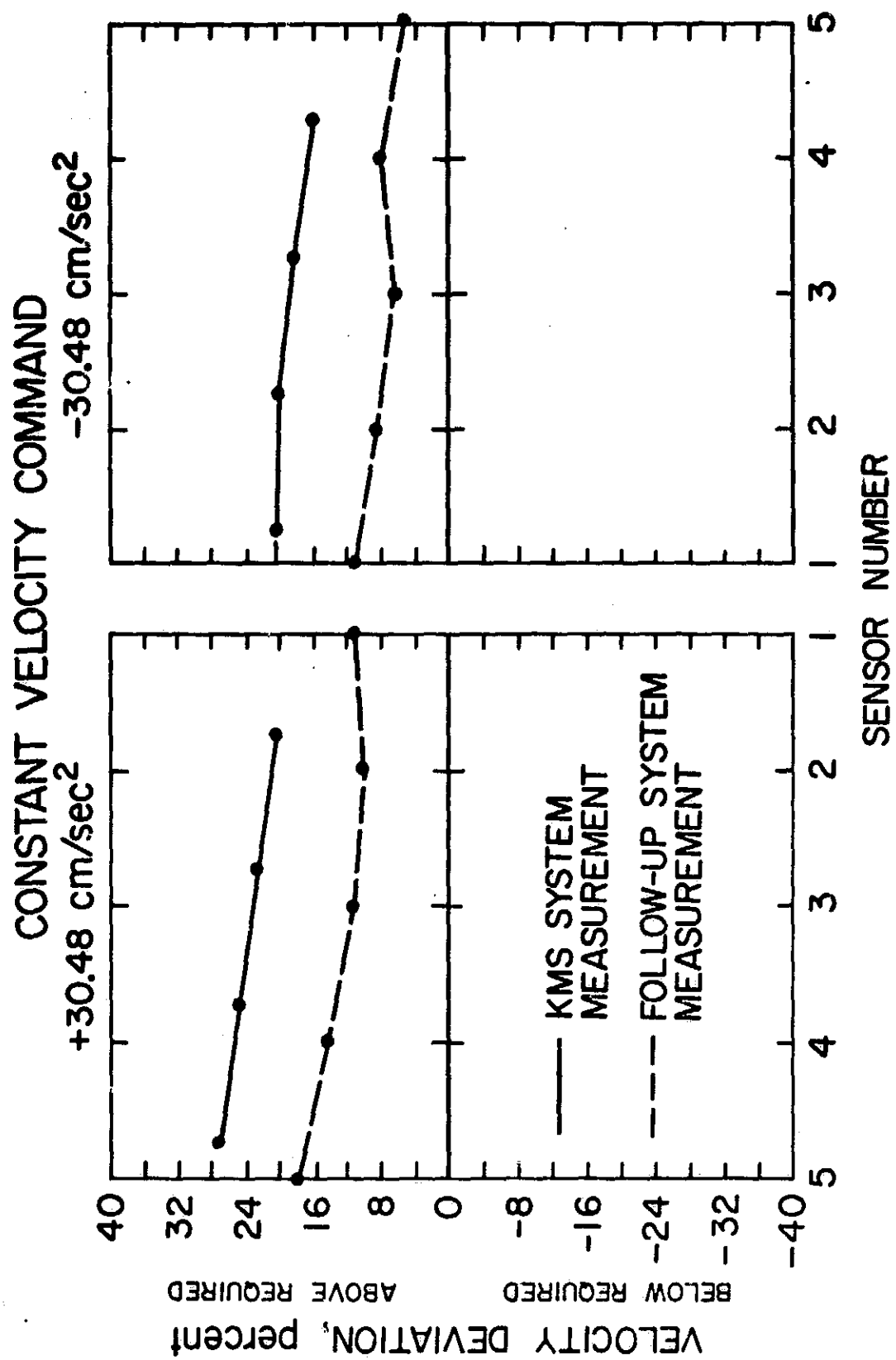


FIGURE 11

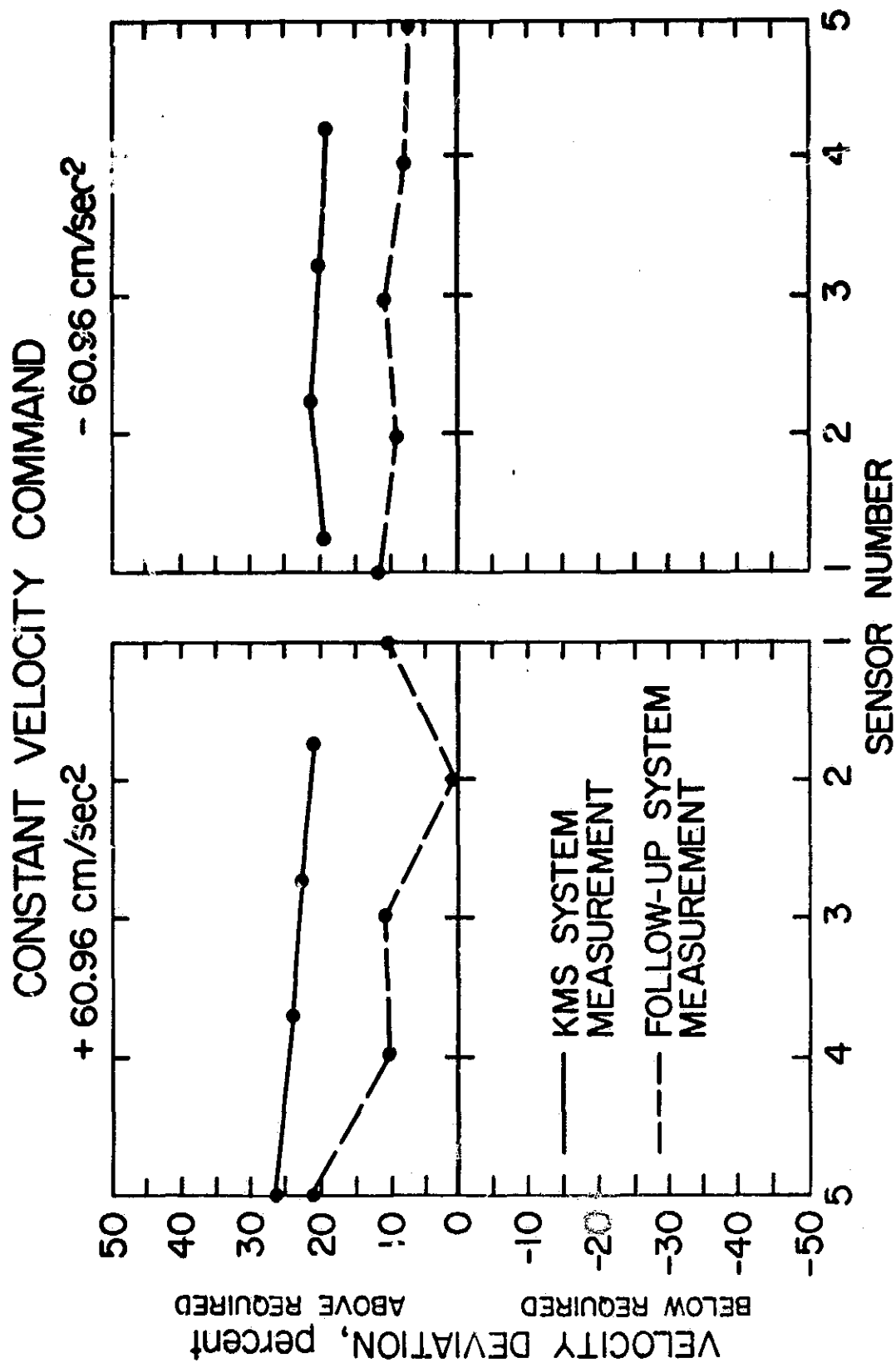


FIGURE 12

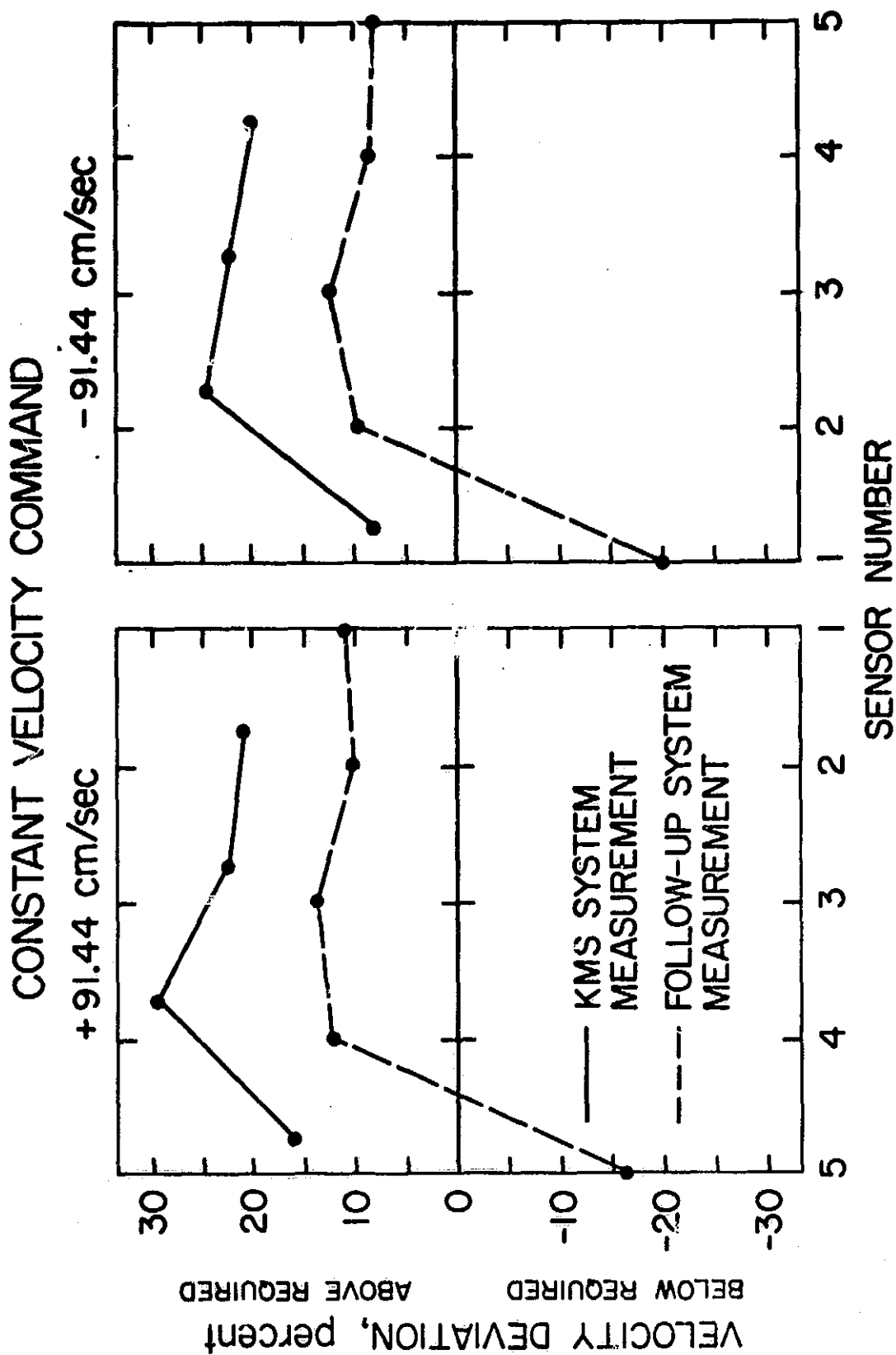


FIGURE 13

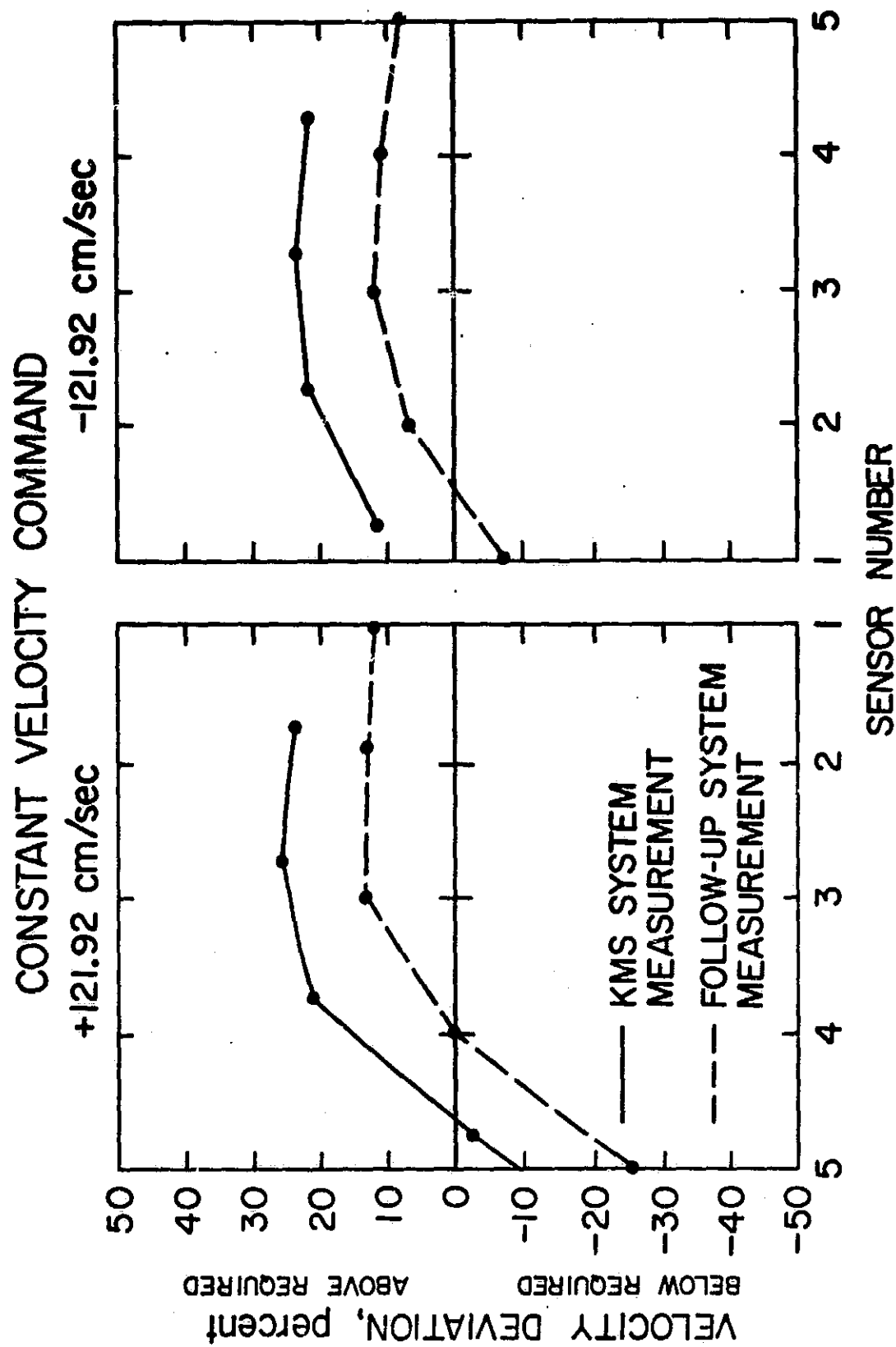


FIGURE 14

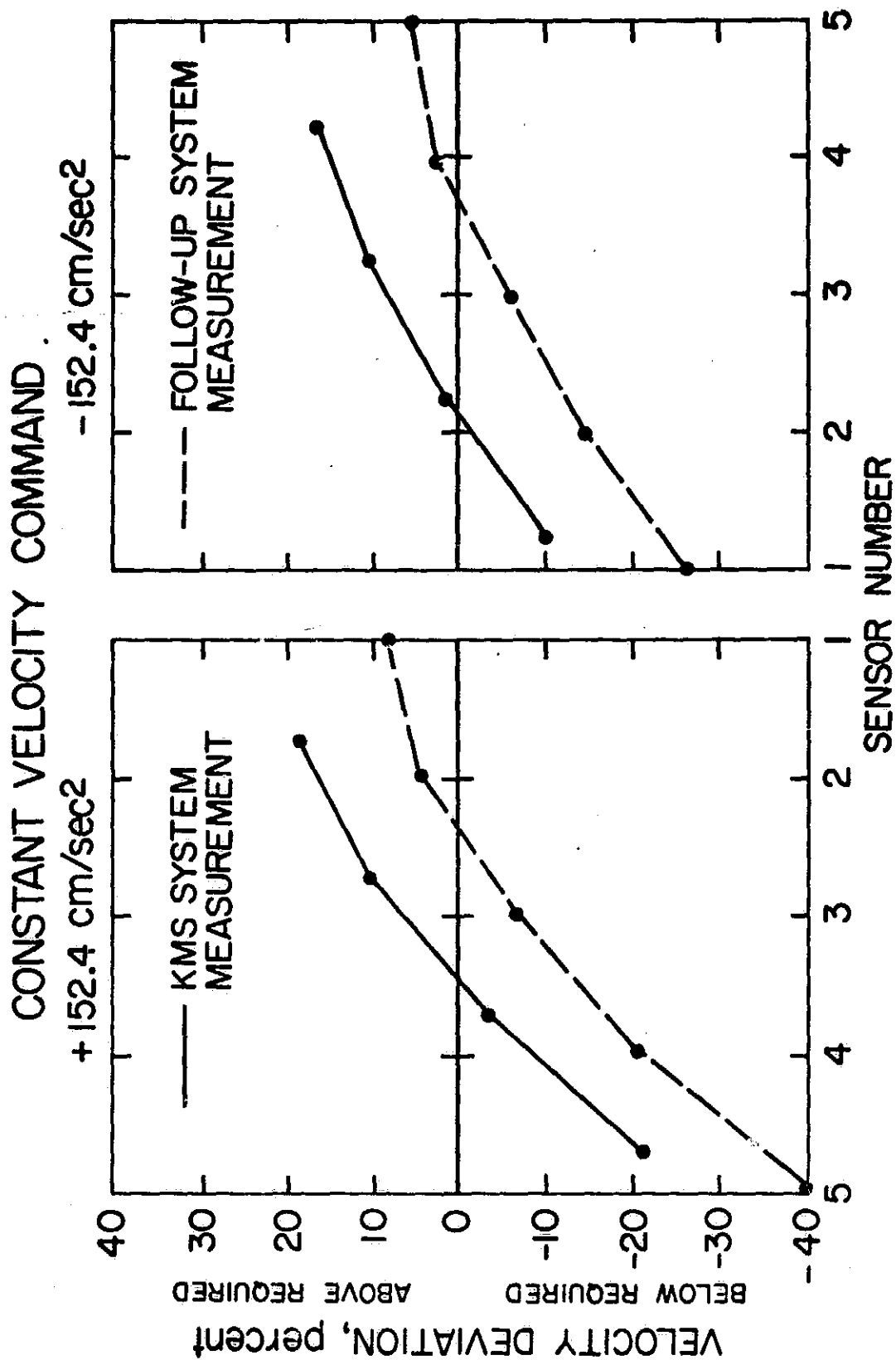


FIGURE 15

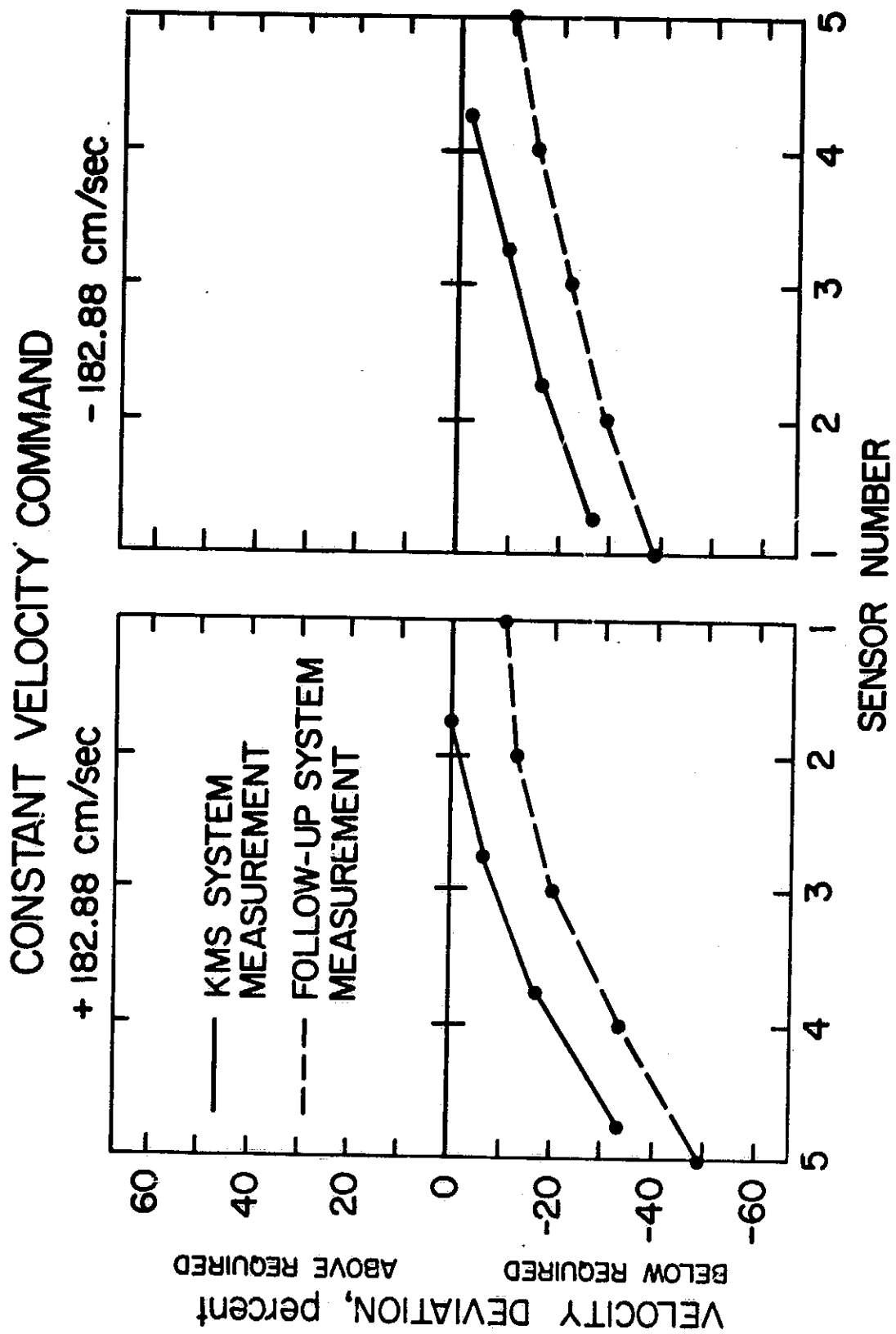


FIGURE 16

lines showing uniform acceleration and motion of the simulator. The accompanying plots of the tachometer readings show occasional discontinuities in almost every case, especially in Figure 9. This may be traceable to noise in the tachometer electrical systems or imperfections in the tachometer mechanical drive which causes jerking. Noise contributions are increasingly less important and noticeable as velocity increases. A comparison of the tachometer readings to KMS values in the graphs show that for all velocities above 15 cm./sec. the general shape and slopes of the two lines are identical. However, KMS values exceed those of the follow-up system by an average of 10%. This may be traced to a scale factor in the tachometer follow-up system and may be easily corrected by rescaling.

Servo Response

For positive velocities below +91 cm./sec., the simulator has overshoot the required velocity by 25% to 50% at the first velocity reading. A linear, negative acceleration brings the velocity closer to the required value as the last sensor is passed. The acceleration is small in this range and can be neglected for positive velocities below +91 cm./sec. If the computer drive equations were rescaled to reflect the velocity error indicated in Figure 17, this region could be defined as the linear operating range of positive velocity. Figure 17 plots the required simulator velocity versus actual simulator velocity. Deviations from the ideal 45° line represent an inaccuracy in the computer-servo system.

For a negative velocity of -3.0 cm./sec., the servo system did not drive the cab at the required speed, but at a rate 14% under that required in the

first sensor space, increasing to 67% under that required at the fourth measurement. This is opposite^{to} the case when the cab moved down, and always drove the simulator above the commanded velocity, although, in both cases the simulator was decelerating in the test area. This may be due to a slight imbalance in the simulator's equilibrators systems requiring the servo system to drive part of the simulator's weight up at slow speed. A relatively linear region would exist at velocities between -15 cm./sec. and -91 cm./sec., if computer drive equations were rescaled to reflect the excess velocity currently encountered in that region as shown in Figure 17.

For velocities in excess of ± 91 cm./sec., the graphs show that the simulator was still accelerating toward the required velocity in the test region. The simulator was barely able to reach +183 cm./sec. and unable to reach -183 cm./sec. in the sensor space. As the required velocity was not attained after almost 198 cm. of travel, and since ± 183 cm./sec. are within specified Z axis velocity limits (± 244 cm./sec.), the conclusion can be reached that a fault exists in the computer-simulator drive system or that the specified limit is too high. In its proper operating state, the simulator should slew from a stop in response to a step input at the maximum permissible acceleration (366 cm./sec.^2 max.) toward the required velocity. At this rate, ± 183 cm./sec. should have been attained from a dead stop in 0.5 seconds. The distance traveled in that time would have been 46 cm., and the simulator would not yet have entered the area of the sensors. Notice that the time of passage in Figure 15 is almost identical to that of Figure 16. It is apparent that an acceleration limit has been reached and that this limit must be signi-

REQUIRED SIMULATOR VELOCITY VS ACTUAL SIMULATOR VELOCITY

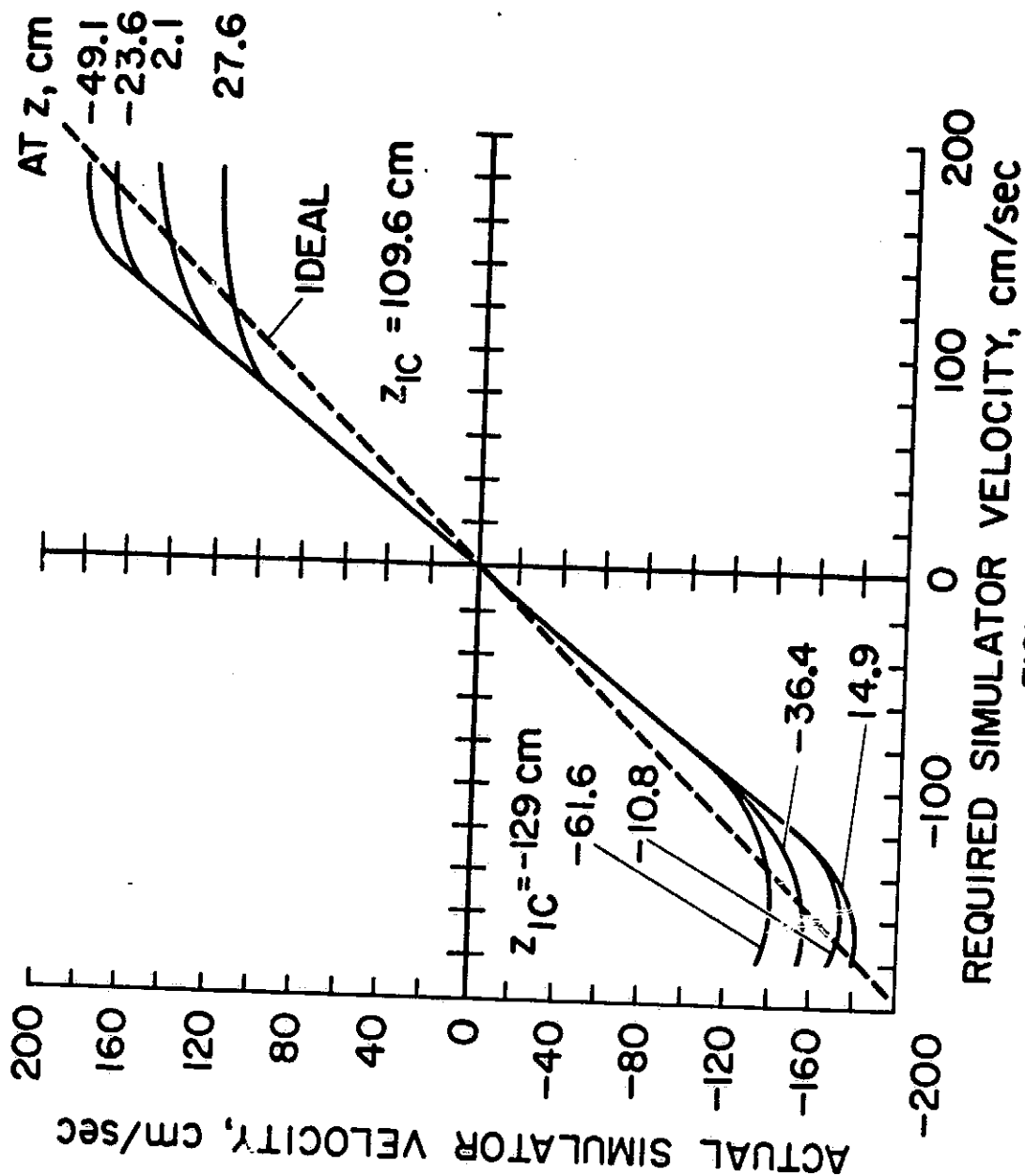


FIGURE 17

ificantly below the $\pm 366 \text{ cm./sec.}^2$ acceleration limit specified for the Z axis. Data taken for velocity requests of $\pm 213 \text{ cm./sec.}$ and $\pm 244 \text{ cm./sec.}$ have not been shown as their graphs are basically identical to Figure 16.

Acceleration Measurement

Figures 18 through 24 display the results of constant acceleration command tests for commands in the range of $\pm 3 \text{ cm./sec.}^2$ through $\pm 183 \text{ cm./sec.}^2$. For constant acceleration requests below 73 cm./sec.^2 , the KMS values for cab acceleration form straight lines of approximately zero slope. The values are generally within 15% of the required value. The performance of the FSAA for acceleration commands in the range of $\pm 73 \text{ cm./sec.}^2$ may be considered linear, accurate, and constant. The accelerometer follow-up signals are very noisy, and differ sharply from the other measurements (see Figures 18 thru 24). As the FSAA drive system and the KMS both agree on FSAA acceleration, it can be concluded that the accelerometer readings in this range are incorrect. The accelerometers used are currently being modified to improve their performance.

Study of the graphs for accelerations in excess of $\pm 73 \text{ cm./sec.}^2$ show that the FSAA acceleration, extrapolated back, reached a maximum outside the sensor range and is decreasing as the cab passes through the sensor space. The FSAA is not currently capable of maintaining accelerations at or in excess of $\pm 110 \text{ cm./sec.}^2$. This is supported by perusal of the accelerometer strip chart graph taken during the tests. This plot shows that the FSAA can reach approximately 213 cm./sec.^2 at the start of a run and that this value falls

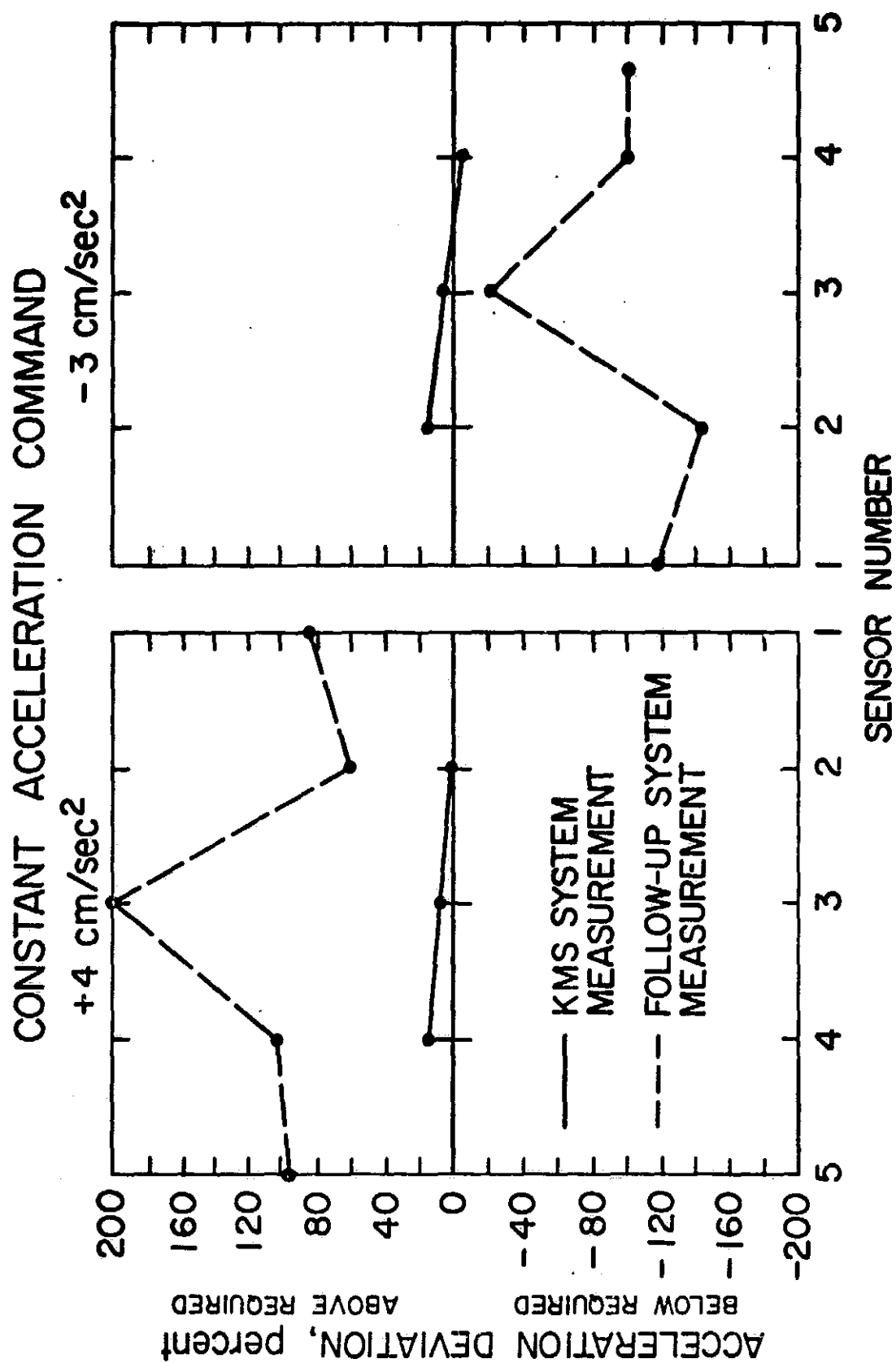


FIGURE 18

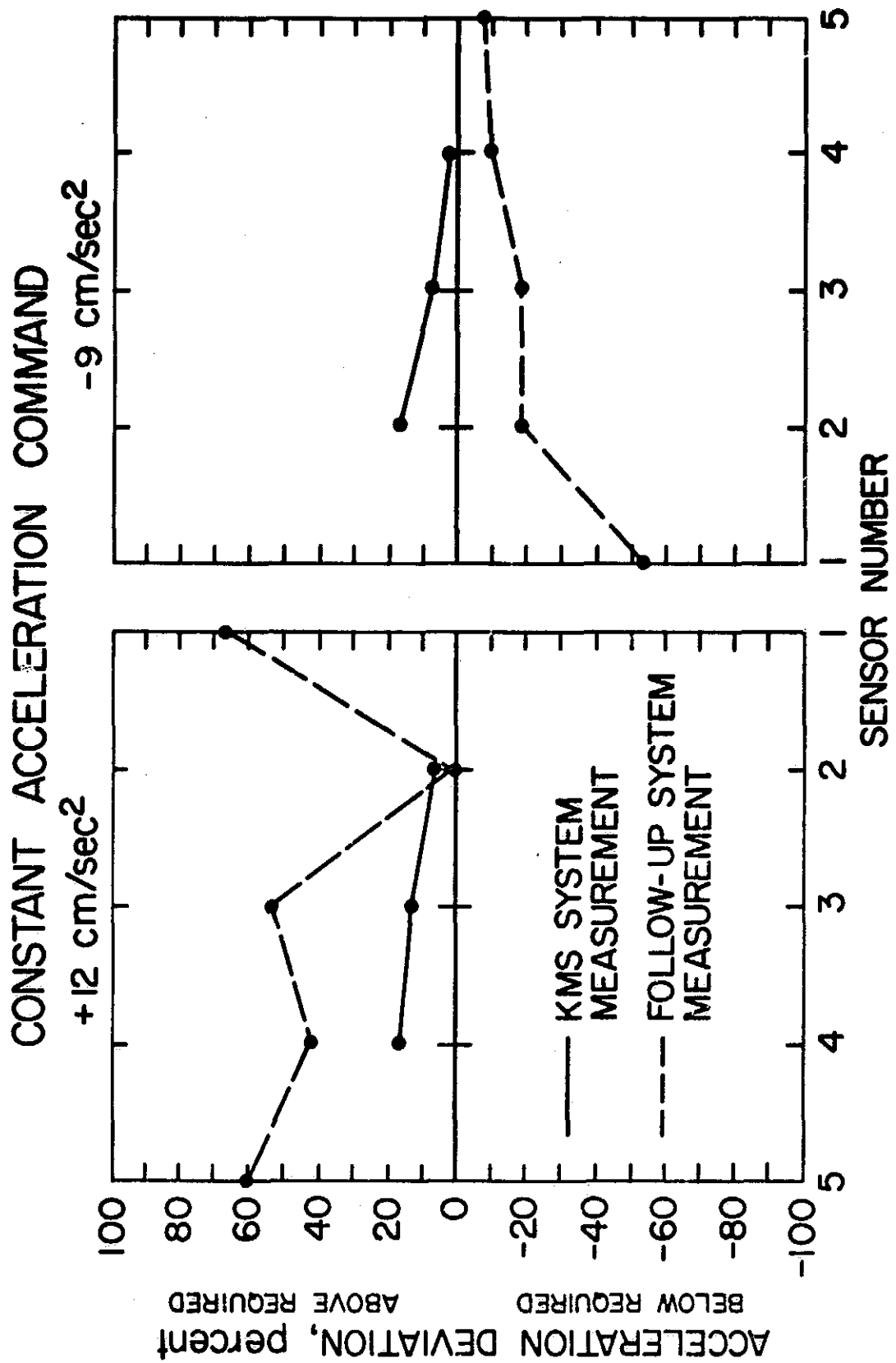


FIGURE 19

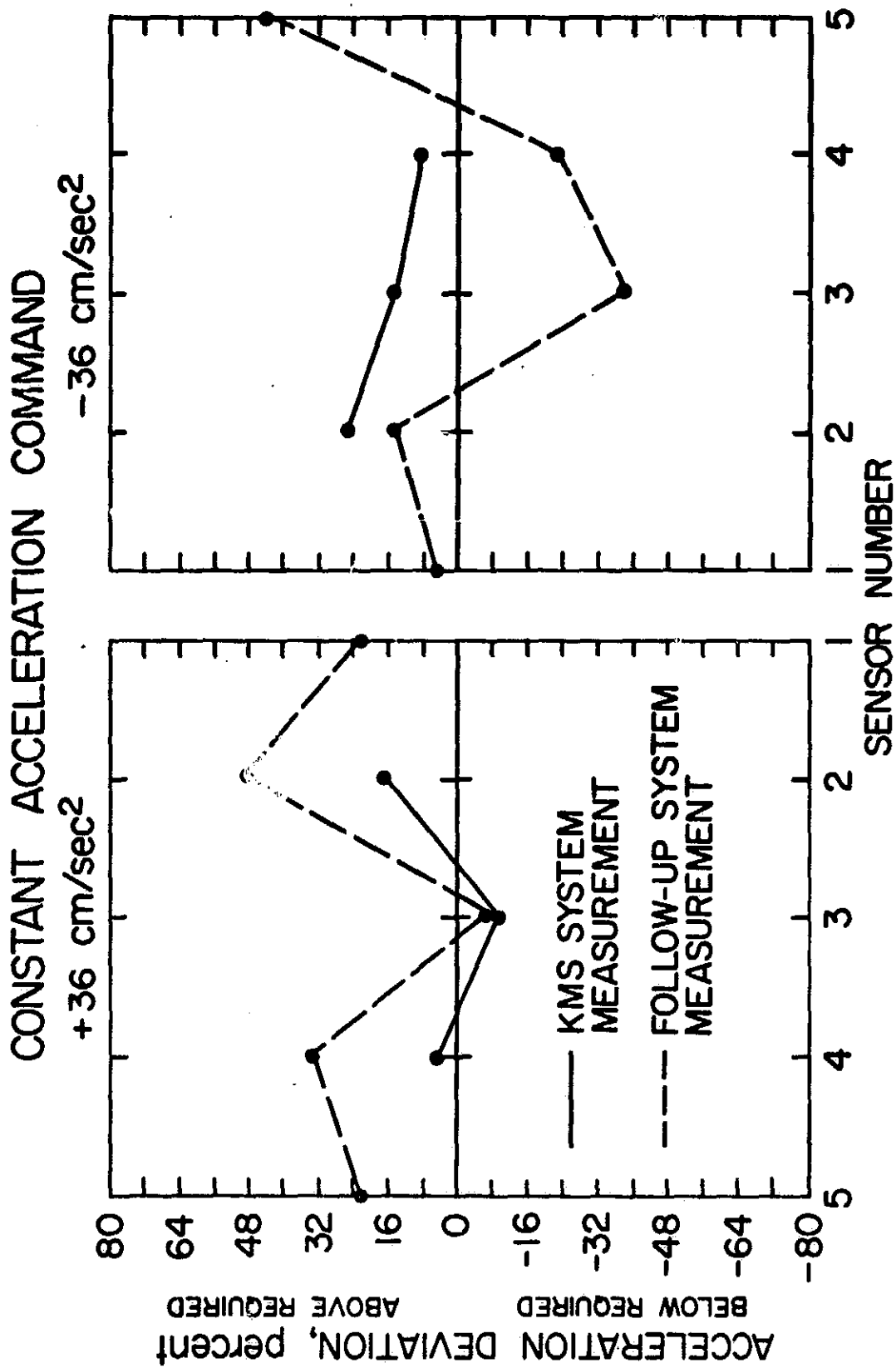


FIGURE 20

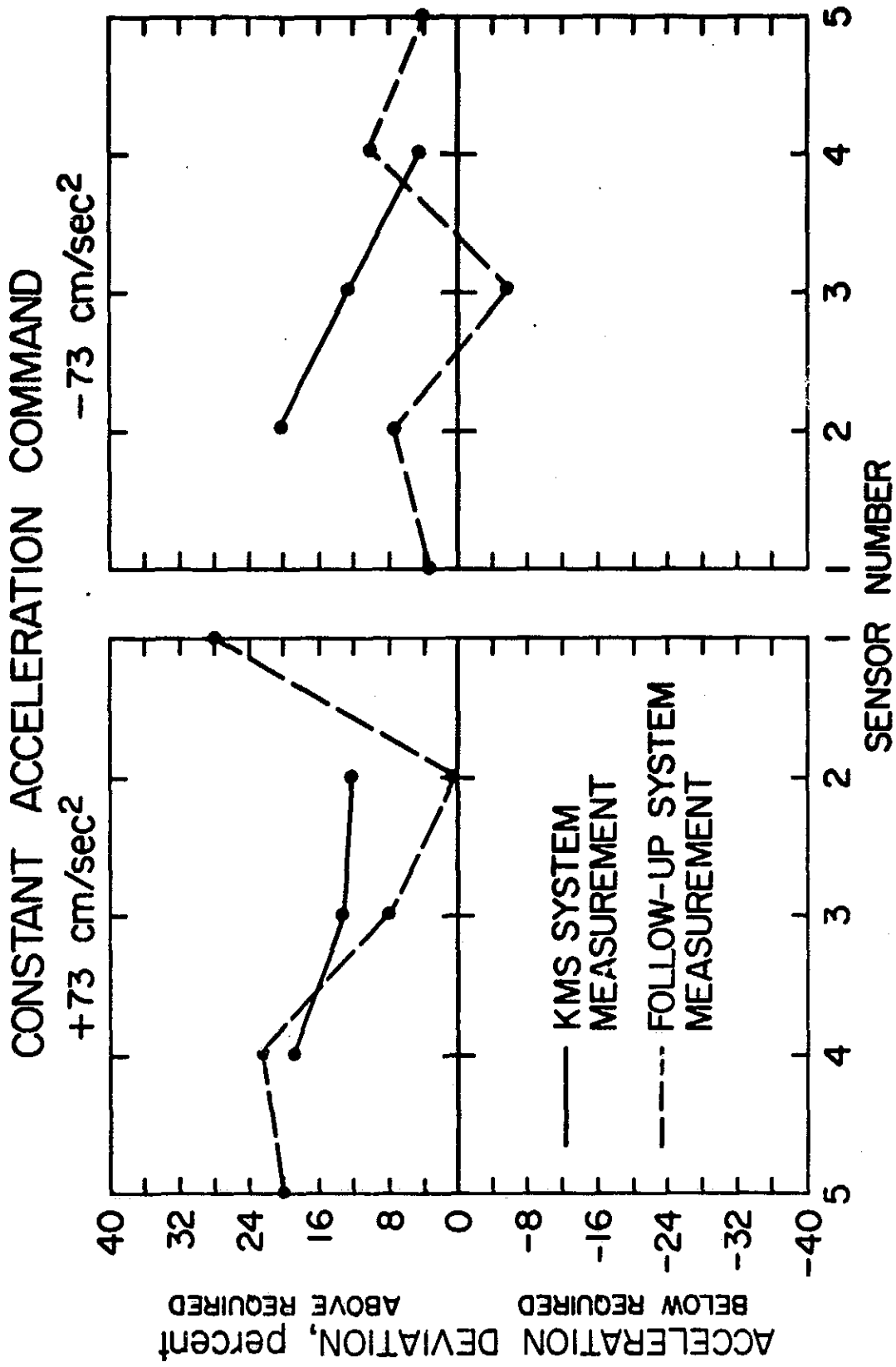


FIGURE 21

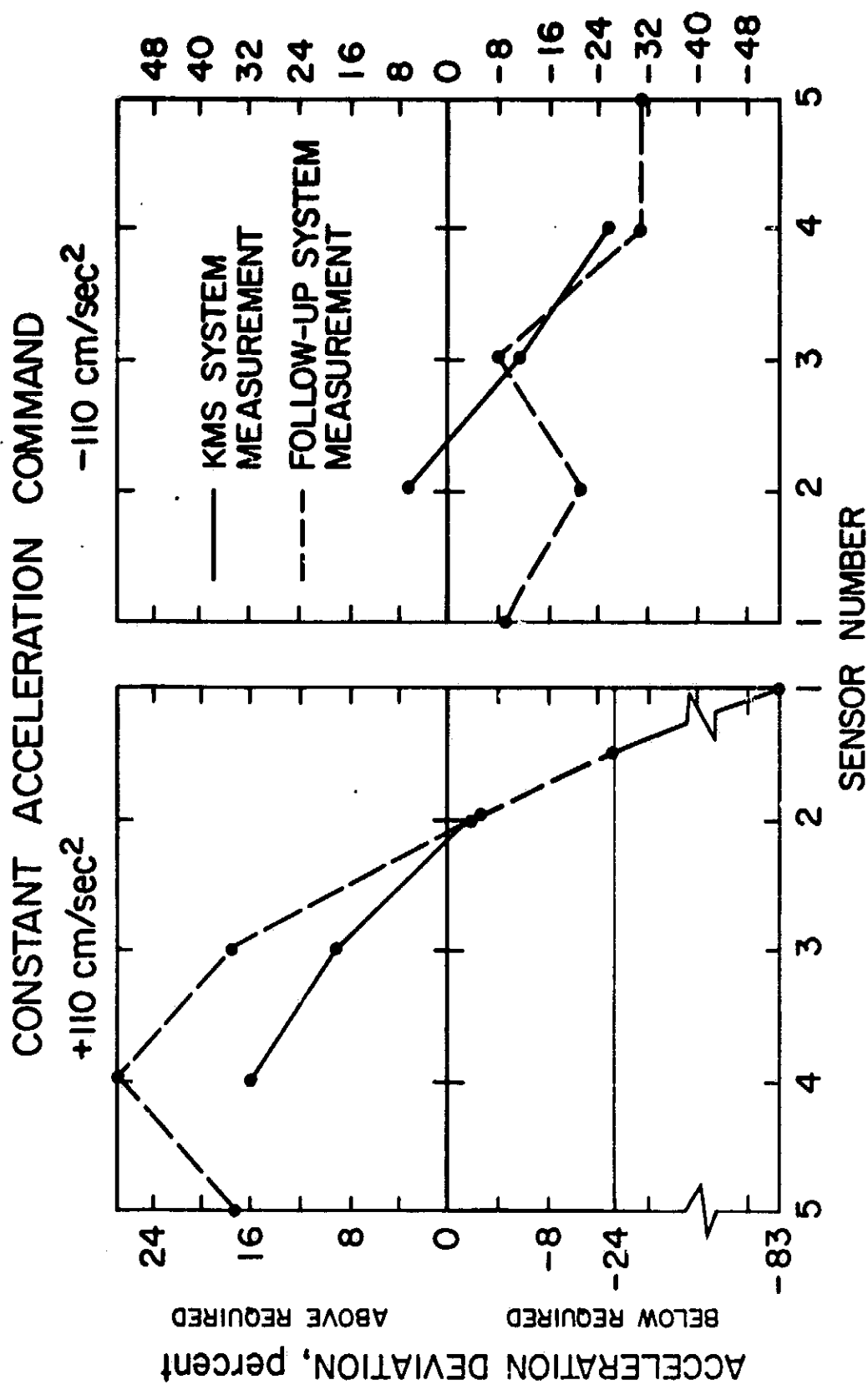


FIGURE 22

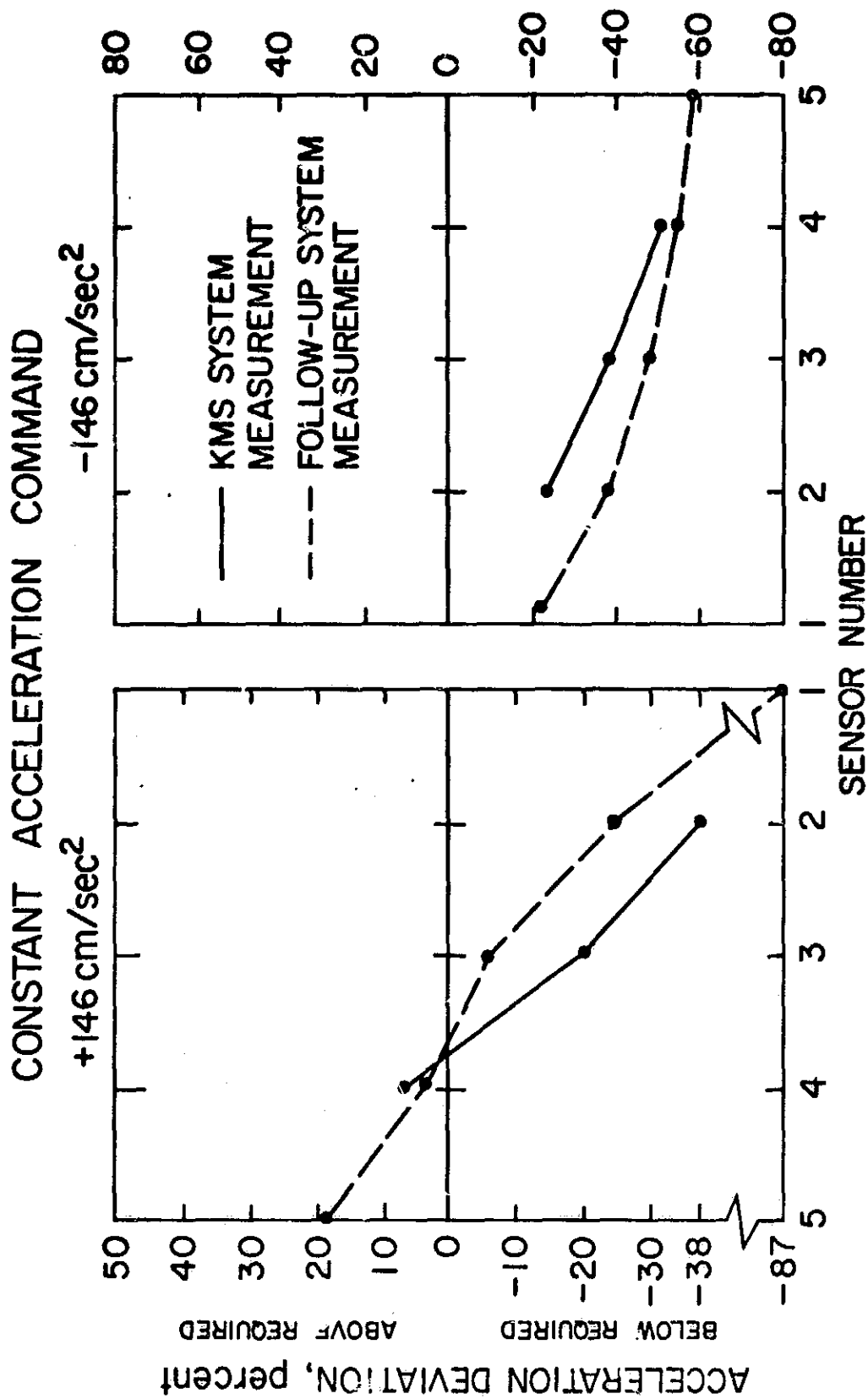


FIGURE 23

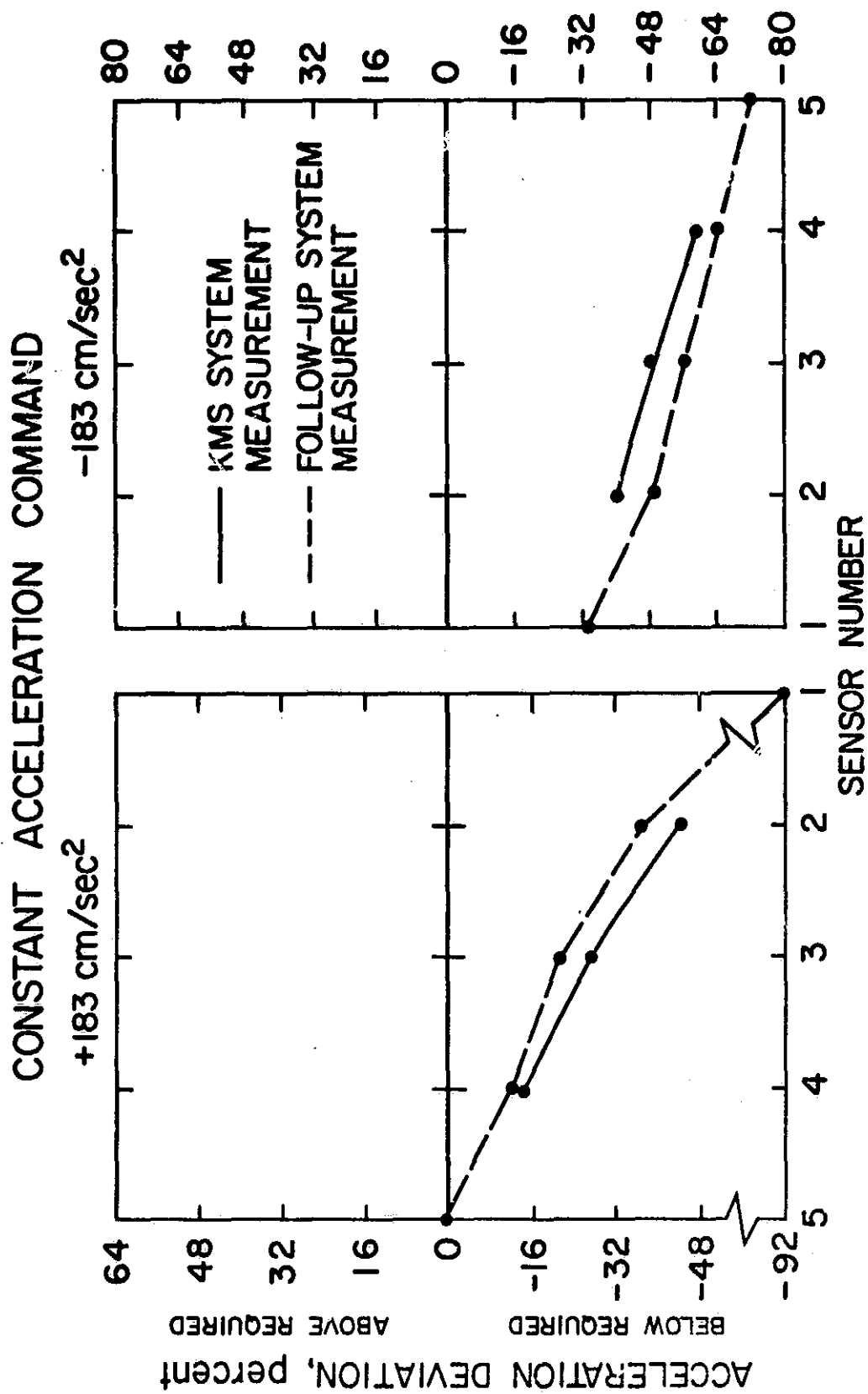


FIGURE 24

off rapidly and linearly as the FSAA passes through the sensors space to a value of about $\pm 91 \text{ cm./sec.}^2$. This lack of attainable and constant accelerations in the area of the specified Z axis acceleration limit of 366 cm./sec.^2 is the reason why constant velocities in excess of $\pm 91 \text{ cm./sec.}$ could not be attained as shown in the velocity section under servo response. Figure 25 is a plot of simulator required acceleration versus actual simulator acceleration. Deviations from the ideal 45° line represents an inaccuracy in the computer-servo system. Note that this deviation is small and could be corrected by rescaling of the computer drive equations for accelerations below 73 cm./sec.^2 . As can be seen, the FSAA is not capable of linear, continuous accelerations in excess of 73 cm./sec.^2 on the Z axis. This may be indicative of machine failure. If not, the acceleration specification for this axis should be revised to reflect actual simulator capacity. This characteristic also has the effect previously noted on attainable simulator Z axis velocity.

Conclusions and Recommendations

These tests, though rudimentary in nature, have shown that the kinematic Measurement System possesses the ability to measure the acceleration, velocity, and position kinematic responses of a motion simulator system, and determine departures in system response from desired motions. From these, corrective maintenance or recalibration may be recommended. Performance parameters which are measurable by the Kinematic Measurement System are:

a. Position

1. Position follow-up circuit linearity, bias, and scale.
2. Position follow-up failure localization.

REPRODUCIBILITY OF THE
ORIGINAL PLOT IS POOR

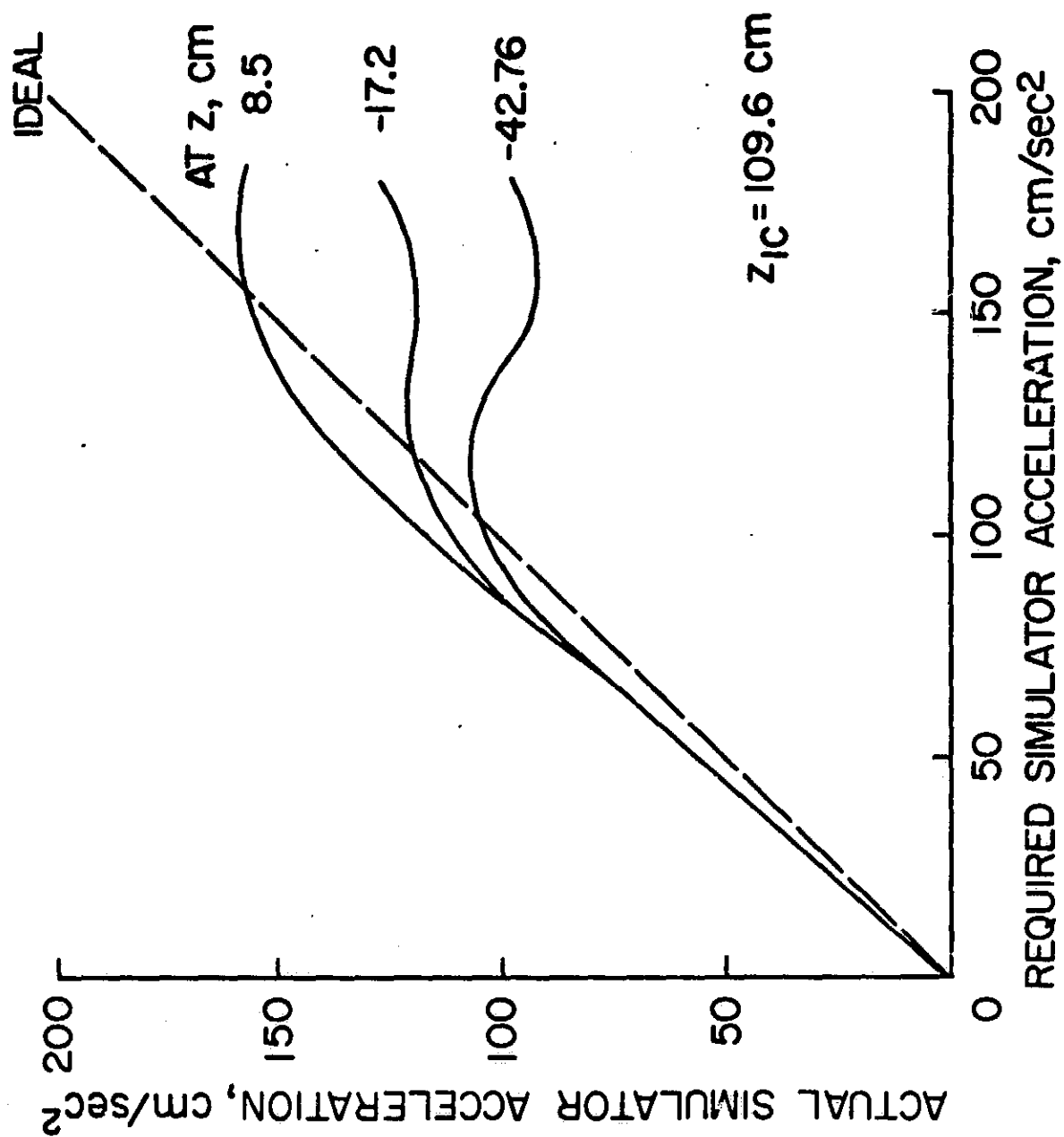


FIGURE 25

3. Position follow-up noise.

- b. Velocity

1. Software bias and scale factors.
2. Velocity drive DAC performance.
3. Servo drive amplifier performance.
4. Servo system responses to step inputs (constant velocity command).
5. Tachometer follow-up linearity, bias, and scale factors.
6. Tachometer follow-up failure localization.
7. Tachometer follow-up noise.
8. Computer drive circuit failure localization.
9. Servo system failure localization.

- c. Acceleration

1. Servo system response to ramp inputs (constant acceleration command).
2. Computer acceleration equation bias and scaling.
3. Accelerometer follow-up linearity, bias, and scale factors.
4. Accelerometer follow-up noise.
5. Accelerometer follow-up failure localization.

More precise measurements could have been made, especially for acceleration, if the number of sensors was increased and the spacing between sensors decreased. This would have significantly increased the sensitivity of the system to small variations of the parameters being measured.

As this technique has shown itself to be a viable method of detecting potential problems in the drive and follow-up systems, as well as providing a

closed loop system calibration technique, it is recommended that the system be expanded to include all axes of motion, and further tested on a motion simulator. More sensors should be added and the space between sensors decreased. Alternatively, further investigation into other methods of sensing simulator position with respect to time should be accomplished. This study should include consideration of low wear continuous systems as well as the discrete types described herein.